ExRET-Opt: An automated exergy/exergoeconomic simulation framework for building energy retrofit analysis and design optimisation

Iván García Kerdan[a, c*], Rokia Raslan[b], Paul Ruyssevelt[a], David Morillón Gálvez[c]

[a] Energy Institute, University College London, 14 Upper Woburn Pl, London, WC1H 0NN, U.K.
[b] Environmental Design and Engineering, University College London, 14 Upper Woburn Pl, London, WC1H 0NN, U.K.

[c] Departamento de Mecánica y Energía, Instituto de Ingeniería, Universidad Nacional Autónoma de México, México, México

Abstract

Energy simulation tools have a major role in the assessment of building energy retrofit (BER) measures. Exergoeconomic analysis and optimisation is a common practice in sectors such as the power generation and chemical processes, aiding engineers to obtain more energy-efficient and cost-effective energy systems designs. ExRET-Opt, a retrofit-oriented modular-based dynamic simulation framework has been developed by embedding a comprehensive exergy/exergoeconomic calculation method into a typical open-source building energy simulation tool (EnergyPlus). The aim of this paper is to show the decomposition of ExRET-Opt by presenting modules, submodules and subroutines used for the framework's development as well as verify the outputs with existing research data. In addition, the possibility to perform multi-objective optimisation analysis based on genetic-algorithms combined with multi-criteria decision making methods was included within the simulation framework. This addition could potentiate BER design teams to perform quick exergy/exergoeconomic optimisation, in order to find opportunities for thermodynamic improvements along the building's active and passive energy systems. The enhanced simulation framework is tested using a primary school building as a case study. Results demonstrate that the proposed simulation framework, provide users with thermodynamic efficient and cost-effective designs, even under tight thermodynamic and economic constraints.

Keywords:
building energy retrofit; exergy; exergoeconomics; building simulation; optimisation.

*Corresponding author at: Energy Institute, University College London, United Kingdom. Tel: +44 (0) 7867798730

E-mail address: i.kerdan.12@ucl.ac.uk (I. Garcia Kerdan)

1. Introduction

Improving building energy efficiency through building energy retrofit (BER) is one of the most effective ways to reduce energy use and associated pollutant emissions. From an economic and environmental perspective, energy conservation and efficiency measures could hold greater potential than deployment of renewable energy technologies [1]. Computational modelling and simulation plays an important role in understanding complex interactions. Building performance modelling and simulation is a fast flourishing field, focusing on reliable reproduction of the physical phenomena of the built environment [2]. Several retrofit-oriented simulation tools have been developed in the last two decades, commonly using as the main energy calculation engine open source tools such as DOE 2.2® [3] and EnergyPlus® [4]. Among the most recent developments are ROBESim [5], CBES [6] and SLABE [7]. Rysanek and Choudhary [8] developed an exhaustive retrofit simulation tool by coupling the transient simulation tool TRNSYS® [9] with MatLab® [10], having the capability to simulate large set of strategies under economic uncertainty.

Additionally, building energy design optimisation, an inherently complex, multi-disciplinary technique, which involves many disciplines such as mathematics, engineering, environmental science, economics, and computer science [11], is being extensively used in building design paractice. Attia et al. [12] found that 93% of multi-objective optimisation (MOO) research is dedicated to early design; however, some studies have also demonstrated the strength of MOO for BER projects [13-15]. Improvement of the envelope, HVAC equipment, renewable generation, controls, etc., while optimising objectives, such as energy savings, occupant comfort, total investment, and life cycle cost have been investigated. Among the most notable contributions in applying MOO to BER design was Diakaki et al. [16]. The authors investigated the feasibility of applying MOO techniques to obtain energy-efficient and cost-effective solutions, with the objective of including the maximum possible number of measures and variations in order to facilitate the project decision making. To date, the most popular available MOO simulation tools are GenOpt, jEPlus, Tpgui, Opt-E-Plus, and BEOpt. Taking the advantages from these tools, retrofit-oriented optimisation studies have become more common in the last decade, considering different decision variables (retrofit measures), objective functions, and constraints, while also investigating a wide range of mathematical algorithms.

2. Exergy and exergoeconomics

2.1 Exergy and buildings

Although widely accepted at scientific and practical levels in building energy design, typical energy analysis (First Law of Thermodynamics) can have its limitations for an in depth understanding of energy systems. Energy analysis cannot quantify real inefficiencies within adiabatic processes and considers energy transfers and heat rejection to the environment as a system thermodynamic inefficiency [17]. The main limitation of the First Law is that it does not account for energy quality, where thermal, chemical, and electrical energy sources, should not be valued the same, since they all have different characteristics and potentials to produce work. Thereby, as a result of a notorious lack of thermodynamic awareness among buildings' energy design, these presents poor thermodynamic performance with overall efficiencies around 12% [18, 19]. Exergy, a concept based on the Second Law of Thermodynamics, represents the ability of an energy carrier to perform work and is a core indicator of measuring its quality. Therefore, the main difference between the First and the Second Law is the capabilities of the latter to account for the different amount of exergy of every energy source while also calculate irreversibilities or exergy destructions.

In some sectors, such as cryogenics [20], power generation [21], chemical and industrial processes [22-23], and renewable energy conversion systems [24], exergy methods count with a certain degree of maturity that makes the analysis useful in everyday practice. Some of these methodologies have been supported with the development of simulation tools, especially in the process engineering field. Montelongo-Luna et al. [22] developed an open-source exergy calculator by integrating exergy analysis into Sim42®, an open-source chemical process simulator. The tool has the potential to be applied into the early stages of process design and/or retrofitting of industrial processess with the aim of locating sources of inefficiencies. Querol et al. [23] developed a Visual Basic add-onn to perform exergy and thermoeconomic analysis with the support of Aspen Plus®, a commercial chemiclal process simualtion software. The aim was to aid the design process with an easy to use interface that allows the engineer to study different alternatives of the same process. Later, Ghannadzadeh et al. [25] integrated an exergy balance for chemical and thermal processes into ProSimPlus®, a process simualtor for energy efficiency analysis. The authors were capable of embedding the exergy subroutines within the commercial tool without the necessity of external software, making the design process easier for the engineer.

However, in buildings energy research, exergy analysis has been implemented at a slower rate, and it is almost non-existent in the industry [26]. A limited number of building exergy-based simulation tools have been developed with the intention to promote the concept of exergy to a broader audience, especially directed towards educational purposes, common practitioners, and decision makers. The first exergy-based building simulation tool can be traced back to the work of the IEA EBC Annex 37 [27], where an analysis tool capable of calculating exergy flows for the building energy supply chain was created. The tool was based on a spreadsheet built up in different blocks of sub-systems representing each step of the building energy supply chain. Based on this development, Sakulpipatsin and Schmidt [28] included a GUI oriented towards engineers and architects. Later, for the IEA EBC Annex49

[29], the tool was improved along with the creation of other modules (S.E.P.E. and DVP). The tool, called the '*LowEx pre-design tool'*, is also a steady-state excel-based spreadsheet, but enhanced with the use of macros and a more robust database for the analysis of more system options. Schlueter and Thesseling [30] developed the GUI, with a focus to integrate exergy analysis into a Building Information Modelling (BIM) software. Other modelling tools have been developed for research purposes, where quasi-steady state or dynamic calculations have been applied mainly with the support of TRANSYS simulation software [31, 32]. However, these tools were developed to cover specific research questions and were not capable of rapidly reproducing their capabilities for different designs.

2.2 Exergoeconomics, optimisation and buildings

Exergy analysis is a powerful tool to study interdependencies, and it is common that exergy destructions within components are not only dependant on the component itself but on the efficiency of the other system components [33]. Rocco et al. [34] concluded that the extended exergy accounting method is a step forward to evaluate resource exploitation as it includes socio-economic and environmental aspects expressed in exergy terms. By applying this concept as optimisation parameter in a generic system, it provides a reduction of overall resource consumption and larger monetary savings when compare to traditional economic optimisation.

Exergy destructions or irreversibilities within the components have some cost implications, therefore, would have an environmental and economic effect on the output streams. As exergy is directly related to the physical state of the system, any negative impact would have an exergy cost which leads to a more realistic appraisal than solely based on monetary costs. Therefore, it can be said that exergoeconomics, and not simple economics (monetary cost), relates better to the environmental impacts. Exergoeconomics can be an effective method for making technical systems efficient by finding the most economical solution within the technically possible limits [35]. In exergoeconomic analysis, depletion of high quality fuels combined with low thermodynamic efficiencies is highly penalised, especially if the required energy demand does not match the energy quality supply.

Among recent studies using exergoeconomics, Kohl et al. [36] investigated the performance of three biomass-upgrading processes (wood pellets, torrefied wood pellets and pyrolysis slurry) integrated into a municipal CHP plant. From an exergy perspective wood pellets was the most efficient option; however, exergoeconomically, the pyrolysis slurry (PS) gives the highest profits with a robust reaction against price fluctuations. With the projected future prices, PS integration allows for the highest profit which a margin 2.1 times higher than for a stand-alone plant without biomass upgrading. Mosaffa and Garousi Farshi [37] used exergoeconomics to analyse a latent heat thermal storage unit and a refrigeration system. The charging and discharging process of three different PCM were analysed form a second-law perspective. Due to lowest investment cost rate of 0.026 M$ and lowest amount of CO_2 emission, the PCM S27 with a length of 1.7m and a thickness of 10mm provided the lowest total cost rate for the system (4094 $/year). Wang et al. [38] applied exergoeconomics to analyse two cogeneration cycles (sCO_2/tCO_2 and sCO_2/ORC) in which the waste heat from a recompression supercritical CO_2 Brayton cycle is recovered for the generation of electricity. Different ORC fluids were considered in the study (R123, R245fa, toluene, isobutane, isopentane and cyclohexane). Exergy analysis reveals that the sCO_2/tCO_2 cycle has comparable efficiency with the sCO_2/ORC cycle; however, when using exergoeconomics, the total product unit cost of the sCO_2/ORC is slightly lower, finding that the isobutane has the lowest total product unit cost (9.60 $/GJ).

2.2.1 Exergoeconomic optimisation

An essential step when formulating exergoeconomic optimisation studies is the selection of design variables that properly define the possible design options and affect system efficiency and cost effectiveness [39]. Research have shown the importance of genetic algorithms (GA) in energy design practice. GA combined with exergoeconomic optimisation has been extensively used in thermodynamic-based research long time before. For example, Valdés et al. [40] used thermoeconomics optimisation and GA to minimise production cost and maximise annual cash flow of a combined cycle gas turbine. Mofid and Hamed [41] applied exergoeconomic optimisation to a 140 MW gas turbine power plant taken as decision variables the compressor pressure ratio and isentropic efficiency, turbine isentropic efficiency, combustion product temperature, air mass flow rate, and fuel mass flow rate. Optimal designs showed a potential to increase exergetic efficiency by 17.6% with a capital investment increase of 8.8%. Ahmadi et al. [42] applied a NSGA-II using exergy efficiency and total cost rate of product as objective functions to determine best parameters of a multi-generation system capable of producing several commodities (heating, cooling, electricity, hot water and hydrogen) Dong et al. [43] applied multi integer nonlinear programming (MINLP) and GA-based exergoeconomic optimisation for a heat, mass and pressure exchange water distribution network. A modified state space model was developed by the definition of superstructure. However, the authors found that due to large number of variables, the GA was not efficient to produce optimal results in a time-effective manner. Sadeghi et al. [44] optimised a trigeneration system driven by a SOFC (solid oxide fuel cell) considering the system exergy efficiency and total unit cost of products as objective functions recommending that the final design should be selected from the Pareto front. Baghsheikhi et al. [45] applied real-time exergoeconomic optimisation in form of a fuzzy inference system (FIS) with the intention to maximise the profit of a power plant at different loads by controlling operational parameters. It was shown that the

FIS tool is faster and more accurate than the GA. Deslauriers et al [46] applied exergoeconomic optimisation to retrofit a low temperature heat recovery system located in a pulp and paper plant. The results showed significant steam operation cost reduction of up to 89% while reducing exergy destructions by 82%, giving the designer more options to be considered than traditional heat exchanger design methods. Xia et al [47] applied thermoeconomic optimisation of a combined cooling and power system based on a Brayton Cycle (BC), an ORC and a refrigerator cycle for the utilisation of waste heat from the internal combustion engine. The authors considered five key variables (compressor pressure ratio, compressor inlet temperature, BC turbine inlet temperature, ORC turbine inlet pressure and the ejector primary flow pressure) obtaining the lowest average cost per unit of exergy product for the overall system. Recently, Ozcan and Dincer [48] applied exergoeconomic optimisation of a four step magnesium-chlorine cycle (Mg-Cl) with HC1 capture. A thermoeconomic optimization of the Mg-Cl cycle was conducted by using the multi-objective GA optimisation within MATLAB. Optimal results showed an increase in exergy efficiency (56.3%), and a decrease in total annual plant cost ($409.3 million). Nevertheless, a big limitation of these studies is the lack of an appropriate decision support tool for the selection of a final design, leaving the decision to the judgement of the engineering.

2.2.2 Exergoeconomics applied to building energy systems

Despite the exergy-based building research developed in the last decade, the application of exergoeconomics and exergoeconomic optimisation research oriented to buildings is limited. The research from Robert Tozer [49, 50] can be regarded as the first buildings-oriented thermoeconomic research showing its practical application to buildings' services. The author presented an exergoeconomic analysis of different type of HVAC systems, locating those that provide best thermodynamic performance. Later, Ozgener et al. [51] used exergoeconomics to model and determine optimal design of a ground-source heat pump with vertical U-bend heat exchangers. Ucar [52] used exergoeconomic analysis to find the optimal insulation thickness in four different cities/climates in Turkey, using reference temperatures for the analysis ranging from -21 °C to 3 °C. It was found that exergy destructions are minimised with increasing insulation and ambient temperatures, but maximised with the increase of relative indoor humidity. The variation of reference temperatures highly affects the thermoeconomic outputs as these are strongly linked to exergy parameters, demonstrating the necessity to be very careful if the analysis is performed using static or dynamic reference temperature [53]. Baldvinsson and Nakata [54] and Yücer and Hepbasli [55] applied the specific exergetic cost (SPECO) method for the analysis of different heating systems. Recently, Akbulut et al. [56] applied exergoeconomic analysis to a GSHP connected to a wall cooling system calculating exergy cost ranges for the compressor, condenser, undersoil heat exchanger, accumulator tank and evaporator, finding an exergoeconomic factor value of the energy system of 77.68%.

Nevertheless, exergoeconomics can never replace long experience and knowledge of technical economic theory. Therefore, tailored methods combining these approaches must be developed. Exergy-based building simulation tools, despite having been created in the past decade, lack exergoeconomic evaluation and an orientation to assess retrofit measures. As shown in the literature, exergoeconomic-based multi-objective optimisations have proven to be valuable for early design and retrofit projects in power plants and chemical processes with common optimisation objectives such as cost, fuel cost, exergy destructions, exergy efficiency, and CO_2 emissions; therefore, a potential exists for its implementation in building energy design. As such, the aim of this paper is to expand the current knowledge in building energy simulation and optimisation by presenting the details of ExRET-Opt, a building-oriented exergoeconomic-based simulation framework for the assessment and optimisation of BER designs, by showing the decomposition of the framework, and presenting modules, submodules and subroutines used for the tool's development. Additionally, it is important to show the application of exergoeconomic optimisation to a real case study, hoping that the study would set the foundation for future similar studies.

3. Calculation framework

The basic exergy and exergoeconomic formulae together with an abstraction of the building energy supply chain has been presented in previous publications [57, 58]. In this paper, the methodological calculation has finally been integrated into a software, where the modules details will be presented in the following sections.

3.1 Exergy analysis

To develop a holistic exergy building exergy analysis framework that considers most of the energy systems located in a building, several exergy methodologies have been merged. For the tool, calculations for thermal end uses and for renewable generations were taken from EBC Annex49 [29] and Torio [59] with some modifications; while for electric-based energy flows, the work from Rosen and Bulucea [60]. The developed holistic method provides with comprehensive means to understand the interactions between the building envelope and the building energy services (Fig. 1).

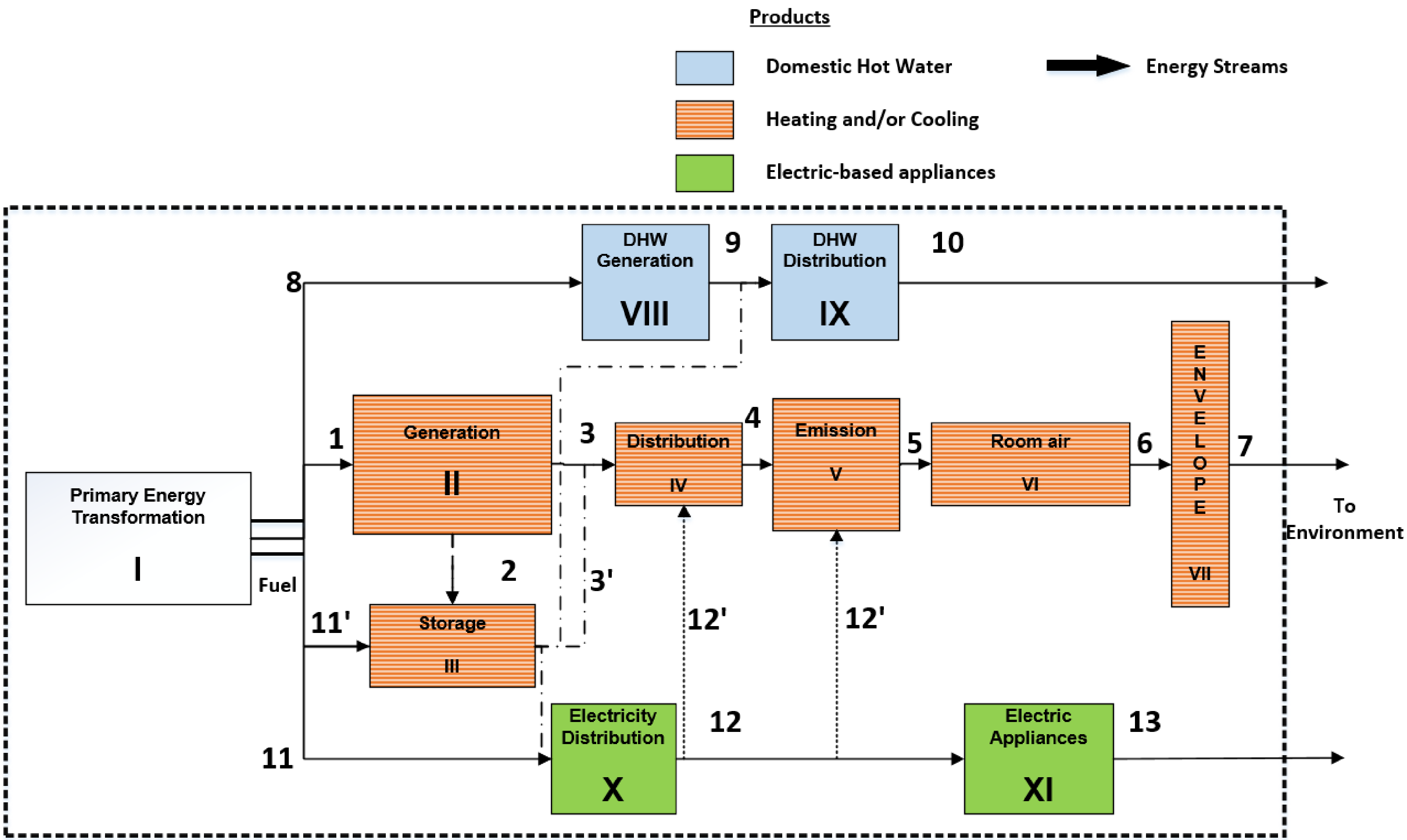

Fig. 1 Thermodynamic abstraction of a generic building energy chain in a building (HVAC, DHW, and electric appliances) [58]

3.2 Exergoeconomic analysis

From a wide range of thermoeconomic methods, the SPECO (specific exergy cost) method [61, 62] was considered ideal for the proposed framework. It is considered the most adaptable framework for BER due to its robustness and widely tested methodology in other energy systems research. The method is based on the calculation of exergy efficiencies, exergy destructions, exergy losses, and exergy ratios (destructions/inputs) at a component and system level, giving the advantage of an ability to locate economically inefficient systems and processes along the whole energy system. After identifying and calculating the exergy streams, the method follows two main steps:

1. definition of fuel and product costs considering input cost, exergy destruction cost, and increase in product costs, and,

2. identification of exergy cost equations.

However, for the SPECO method to be useful in BER design, a novel levelized exergoeconomic index, the *exergoeconomic cost-benefit indicator* $Exec_{CB}$, has been developed. This is calculated as follows:

$$Exec_{CB} = \dot{C}_{D,sys} + \dot{Z}_{sys} - \dot{R} \quad (1)$$

where $\dot{C}_{D,sys}$ is the building's total exergy destruction cost, $\dot{Z}_{sys}$ is the annual capital cost rate for the retrofit measure, and $\dot{R}$ is the annual revenue rate. All three parameters are levelized considering the project's lifetime (50 years) and the present value of money. The outputs are given in £/h. The indicator tries to solve the gap of integrating exergoeconomic evaluation in typical economic analysis for BER design, by expressing exergy losses and its relative cost into an indicator that is straightforward to understand. Specifically, for BER analysis, first, a benchmark value has to be calculated for the pre-retrofitted building. This indicator will only be composed of exergy destruction costs $\dot{C}_{D,sys,baseline}$ ($\dot{Z}_{sys}$=0 and $\dot{R}$=0). After the retrofit analysis is performed, if the retrofitted building presents a $Exec_{CB}$ lower than the baseline $\dot{C}_{D,sys,baseline}$, the design represents both a cost-effective solution and an improvement in exergy performance.

Exergy-efficient and cost-effective → $Exec_{CB} > \dot{C}_{D,sys,baseline}$

Exergy-inefficient and cost-ineffective → $Exec_{CB} < \dot{C}_{D,sys,baseline}$

The proposed exergy/exergoeconomic framework aims to allow the practitioner to quantify the First and Second Law parameters in order to locate more opportunities for improvement. Several steps with different activities exist in common BER practice [63]. The proposed framework, consists of three levels and is illustrated in Fig. 2.

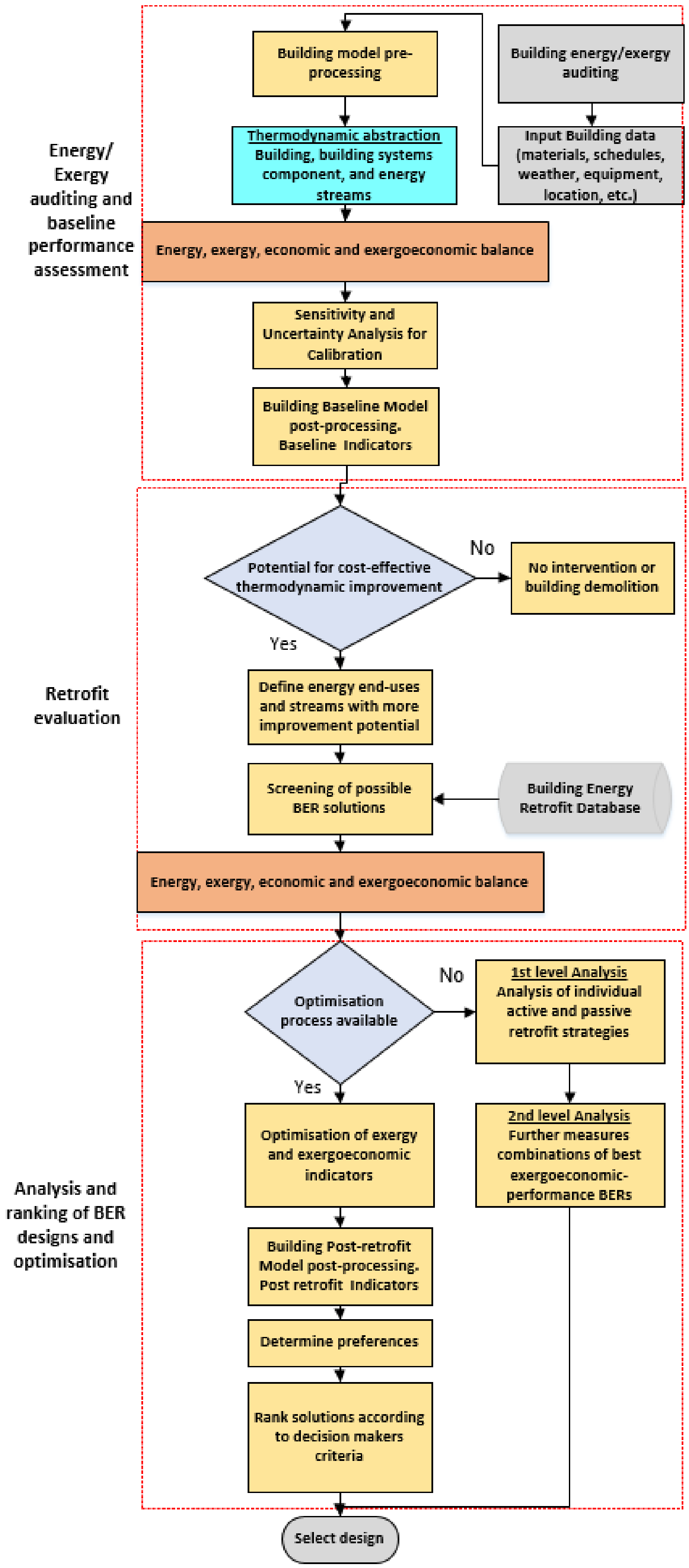

289

290 **Fig. 2 Exergy and exergoeconomic analysis methodology for BER**

4. ExRET-Opt simulation framework

ExRET-Opt, a simulation framework consisting of several software subroutines, was developed combining different modelling environments such as EnergyPlus, SimLab® [64], Python® [65], and the Java-based jEPlus® [66] and jEPlus + EA® [67]. This software was chosen for four main reasons:

a. Open source software that can be modified and adapted according to the research necessities.

b. EnergyPlus was selected for First Law analysis as it is the most widely used building performance simulation programme in academia and industry, allowing simulation of HVAC systems and building envelope configurations.

c. Python programming language is ideal as a *scripting tool* for object-oriented system languages, which also supports post-processing analysis by including data analysis packages.

d. All chosen software has the ability to work with text based inputs/outputs which facilitates the communication between the environments.

ExRET-Opt was designed to be modular and extensible. This framework gives the possibility to study a wide range of BER measures and optimise designs under different objective functions, such as energy and exergy use, exergy destructions and losses, exergy efficiency, occupants' thermal comfort, operational CO_2 emissions, capital investment, life cycle cost, exergoeconomic indicators, etc. The modelling engine is based on different existing modelling environments and five modules:

Module 1. Input data and baseline building modelling

Module 2. Building model calibration

Module 3. Exergy and exergoeconomic analysis (and parametric study)

Module 4. Retrofit scenarios

Module 5. GA optimisation and MCDM

Additionally, ExRET-Opt has three operation modes:

Mode I. **Baseline evaluation:** A dynamic energy/exergy analysis and economic/thermoeconomic evaluation is performed to obtain baseline values and benchmarking data.

Mode II. **Parametric retrofit evaluation:** Using a comprehensive retrofit database, a parametric analysis can be performed for comparison and exploration of a wide range of active and passive retrofit measures

Mode III. **Optimisation:** Considering all possible combinations of retrofit measures, and based on constraints and objectives given by the user, ExRET-Opt can use a genetic algorithm-based optimisation procedure to search for close-to-optimal solutions in a time-effective manner

Depending of the operation mode, ExRET-Opt modules that are active are the following:

Table 1 Active modules depending on ExRET-Opt operating mode

ExRET-Opt	Mode I	Mode II	Mode III
Module 1: Input data and baseline building modelling	x	x	x
Module 2: Building model calibration	x	x	x
Module 3: Exergy and exergoeconomic analysis (and parametric study)	x	x	x
Module 4: Retrofit scenarios		x	x
Module 5: MOGA optimisation and MCDM			x

Following sections will focus on describing these modules in detail by explaining the simulation process involved and the coupling of different software environments and routines.

4.1 Modules and process description

4.1.1 Module 1: Input data and baseline building modelling

First, a pre-processing phase is involved were data collection, with regards to the building physical characteristics, occupancy profiles, energy systems, weather data, and energy prices, should be carried out, in order to construct a pre-calibrated baseline building model. A significant number of data sources is required for this specific task. Most common approaches are site visits and BMS data, which represent the best source of information. When data is missing or is hard to measure (i.e. occupancy levels, envelope thermal characteristics, internal heat gains, etc.), other sources of information, such as CIBSE [68] and ASHRAE [69] guides can be used to support the building modelling process [70]. Fig. 3 illustrates the modelling environments involved within this module.

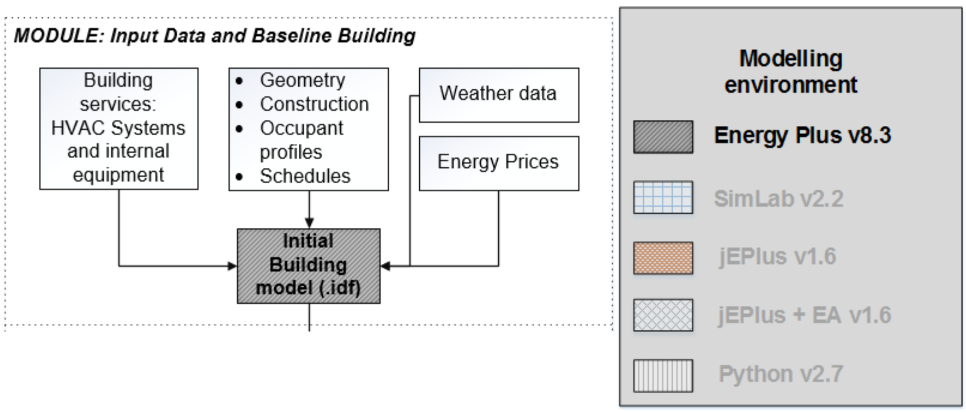

Fig. 3 ExRET-Opt Module 1 simulation process

For the buildings' energy modelling, ExRET-Opt has its foundation on EnergyPlus 8.3. Its biggest strength is the fact that it works with .txt files, which makes it possible to receive and produce data in a generic text files form, making it easy to create third party add-ins.

4.1.2 Module 2: Baseline building model calibration

Considering the effects of uncertainties in building energy modelling, as a second step in the modelling process, ExRET-Opt has included a 'calibration module'. The module was included mainly for deterministic calibration purposes. For the calibration process, a three-software process is required. Apart from EnergyPlus, both SimLab 2.2 and jEPlus 1.6.0 are necessary. SimLab is a software designed for Monte Carlo (MC) based uncertainty and sensitivity analysis, able to perform global sensitivity analysis, where multiple parameters can be varied simultaneously and sensitivity is measured over the entire range of each input factor. On the other hand, JEPlus is a Java-based open source tool, created to manage complex parametric studies in EnergyPlus. Fig. 4 illustrates the module's process.

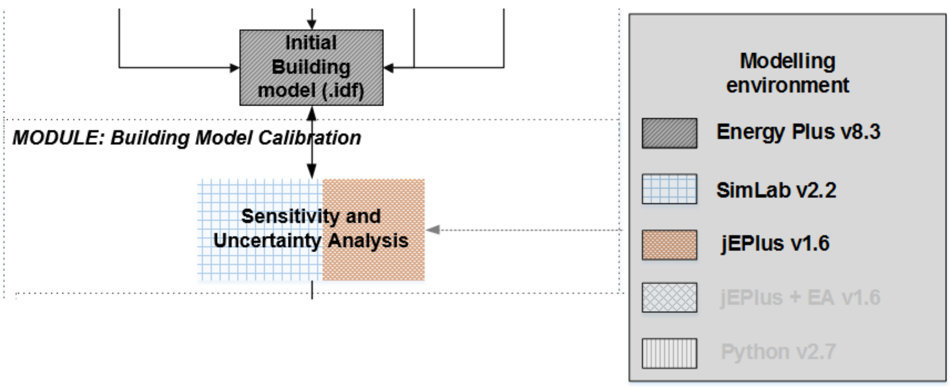

Fig. 4 ExRET-Opt Module 2 simulation process

The sampling method is based on Latin Hypercube Sampling (LHS) in order to keep the number of required simulations at an acceptable level. SimLab creates a spreadsheet with the new sample to be introduced to EnergyPlus. Then, with the aid of jEPlus, ExRET-Opt handles the spreadsheet where the new EnergyPlus building models (.idf files) are created. Following, jEPlus passes the jobs to EnergyPlus for thermal simulation, where parallel simulation is available to make full use of all available computer processors. The final calibrated baseline energy model should meet the requirements of the ASHRAE Guideline 14-2002: *Measurement of Energy Demand and Savings* and is selected by having the lower Mean Bias Error (MBE) and Coefficient of Variation of the Root Mean Squared Error (CVRMSE).

4.1.3 Module 3: Energy/Exergy and Exergoeconomic analysis

Undoubtedly, Module 3 can be considered as the most important main routine within ExRET-Opt. The entire modelling process of Module 3 is based on two subroutines: 'subroutine: *dynamicexergy*' and 'subroutine: *exergoeconomics*'. The code of these subroutines is based on the mathematical formulae described in previous publications and that were further implemented in Python scripts. The strengths of Python programming language and the main reason of its integration in the tool is its modularity, code reuse, adaptability, reliability, and calculation speed [2]. Fig 5 illustrates the interaction among the different modelling environments involved in Module 3.

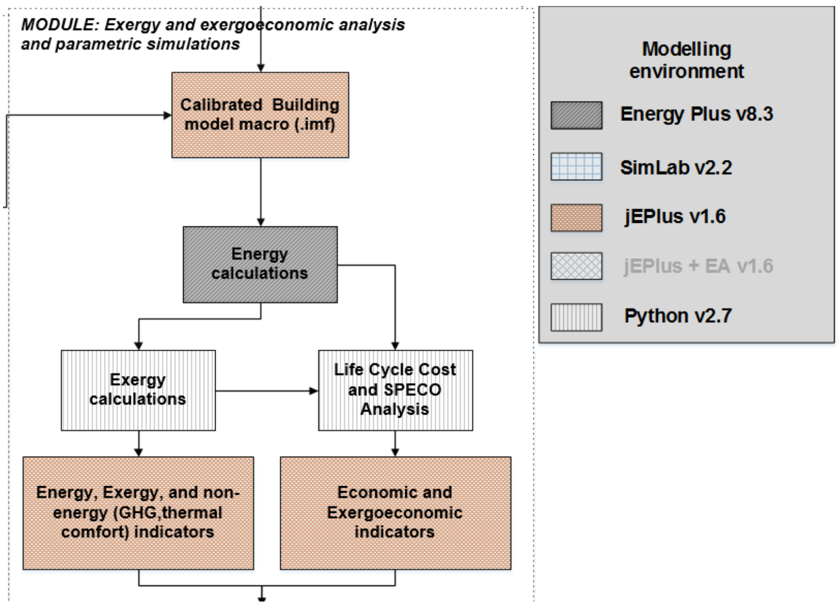

Fig. 5 ExRET-Opt Module 3 simulation process

To further detail the module process, before ExRET-Opt calls the first subroutine, the reference environment has to be specified. As the exergy method only considers thermal exergy, the *.epw* weather file with hourly data on temperature and atmospheric pressure has to be used. Exergy analysis calculated by the 'subroutine: *dynamicexergy',* performs the analysis in the four different products of the building (heating, cooling, DHW, and electric appliances). This procedure is used to split the typical approach of a single stream analysis into multiple streams' analysis, able to calculate exergy indicators of each product in more detail. Following the end of the first subroutine, the 'subroutine: *exergoeconomics'* is called by ExRET-Opt and finally produces all the needed thermodynamic and thermoeconomic outputs.

For the integration of the subroutines into EnergyPlus, jEPlus is required. JEPlus latest versions provide users with the ability to use Python scripting for running own-made processing scripts, where communication between EnergyPlus and the Python-based exergy model is mainly supported through the use of .rvx files (extraction files data structure represented in JSON format). These files also allow the manipulation and handling of data back and forth among EnergyPlus, Python, and jEPlus. The detailed process of joining EnergyPlus and the developed subroutines is illustrated in Fig. 6.

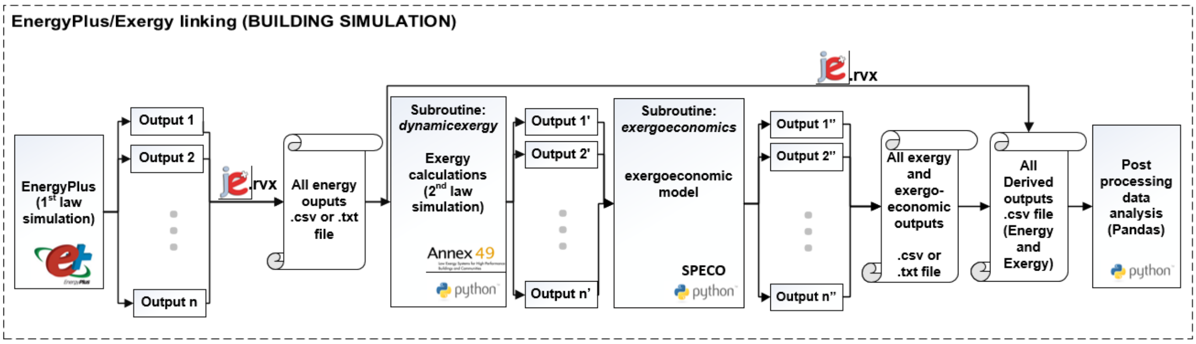

Fig. 6 Flow of Energy/Exergy co-simulation using EnergyPlus, Python scripting and jEPlus

After both, 'subroutine: *dynamicexergy'* and 'subroutine: *exergoeconomics'* are called and calculations are performed, a new spreadsheet version is obtained with all the required outputs. The current version of the model is capable of providing 250+ outputs between energy, exergy, economic, exergoeconomic, environmental, and other non-energy indicators.

4.1.4 Module 4: Retrofit scenarios and economic evaluation

As building energy efficiency can usually be improved by both passive and active technologies, a comprehensive BER database including both technology types was compiled as part of the framework. This module encompasses a variety of retrofit measures (parameters) typically applied to non-domestic buildings in the UK and Europe [71, 72]. The module includes more than 100 individual energy saving measures. Consequently, attached prices are provided per unit (either kW or by m²) since the model automatically calculates the total capital price for either individual or combined measures. The list of technologies, variables, and prices[1] for all retrofit measures are detailed in Appendix A. To reduce economic uncertainties, several other considerations were included in the model such as future energy prices and government incentives (RHI and FiT). Depending on the retrofit technology, this could play a major role in the financial viability of some BER designs. To code each measure, these were implemented by developing individual stand-alone code recognisable ('*.idf* files') by EnergyPlus. Since the manual evaluation of retrofit measures is not feasible, ExRET-Opt uses parametric simulation

[1] If prices for some measures were not in local currency (GBP), conversion rates from 25th-October-2015 were considered.

to manipulate models, modify building model code, and simulate them. By using the EP-Macro function within EnergyPlus and coupling the process with jEPlus, it is possible to handle these 'pieces of code' and introduce them into the main building model (Fig. 7).

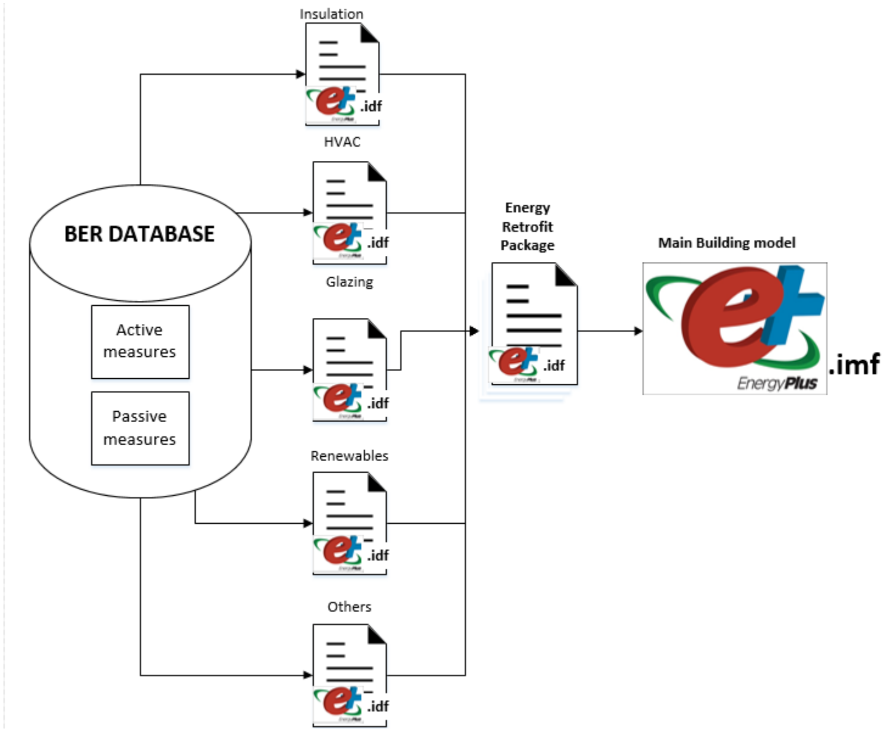

Fig. 7 Building model construction using ExRET-Opt BER database

After the building model is finally constructed with its corresponding retrofit measures, including its techno-economic characteristics, a post-retrofit performance and prediction has to be performed. For this, ExRET-Opt Module 3 'subroutine: *dynamicexergy*' and 'subroutine: *exergoeconomics*', have to be called again. Fig. 8 illustrates the entire process of Module 4.

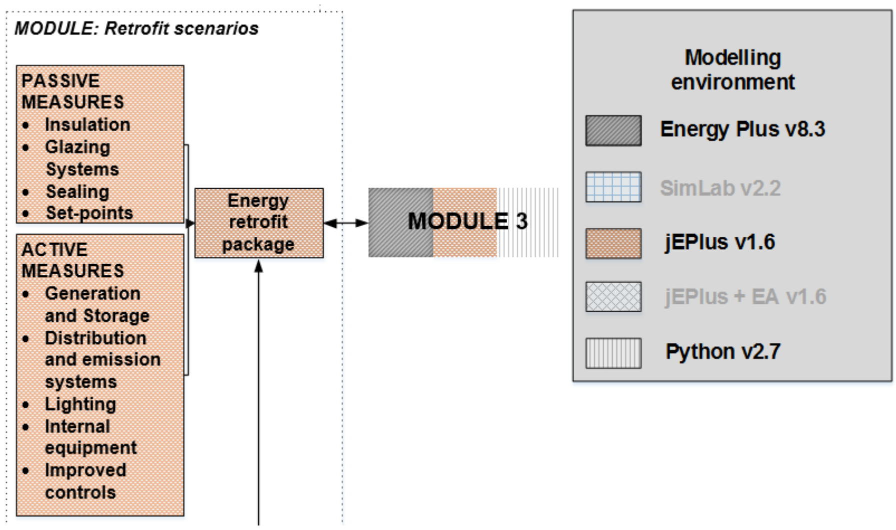

Fig. 8 ExRET-Opt Module 4 simulation process

4.1.5 Module 5: Multi objective optimisation with NSGA-II and MCDM

Modules 3 and 4 have the capability to perform parametric or full-factorial simulations where an automation process of creating and simulating a large number of building models can be done. However, this process has its limitations, mainly depending on time constrains and computing power. For this reason, ExRET-Opt has the option of being used with an optimisation module, able to tackle multi-objective problems, reducing computing time, and achieving sub-optimal results in a time-effective manner.

To couple the framework with the optimisation module, a call function is required to automatically call the different generated building models, process the simulation, and return outputs for the subsequent energy/economic and exergy/exergoeconomic analysis. As seen in Fig. 9, this process is integrated within ExRET-Opt with the help of the Java platform JEPlus+EA. jEPlus+EA provides an interface with little configuration where the necessary controls (population size, crossover rate and mutation rate) are provided in the GUI or can be coded using Java commands. Meanwhile, the communication between platforms is done with the help of the .rvx file (jEPlus extraction file), where, in addition, objective functions and constraints have to be defined.

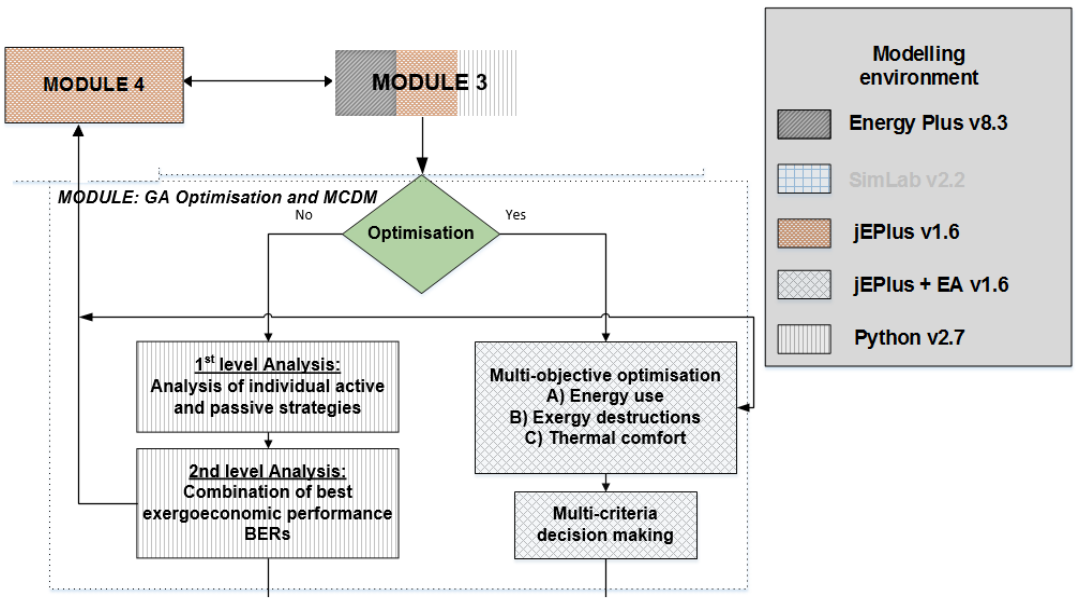

Fig. 9 ExRET-Opt Module 5 simulation process

The advantages of using NSGA-II as the optimisation algorithm, is the ability to deal with large number of variables, ability for continuous or discrete variables' optimisation, simultaneous search from a large sample, and ability for parallel computing [73].

4.1.6 Module 5a: Solution ranking - MCDM submodule

The Pareto front(s) generated by Module 5 provides the decision maker with valuable information about the trade-offs for the objectives involved. A method that can be used at this stage to rank optimal solutions depending on the user's needs is Multi Criteria Decision Making (MCDM). In ExRET-Opt, MCMD was included as a post-processing external module, where Pareto solutions have to be exported to an Excel-based spreadsheet. For ExRET-Opt, similar to Asadi et al. [14], compromise programming (CP) was selected as the MCDM method. CP allows reducing the set of Pareto solutions to a more reasonable size, identifying an ideal or utopian point which serves as a reference point for the decision maker. Thus, the decision model has to be modified by including only one criterion. For this, a distance function has to be analysed to find a set of solutions closest to the ideal point. This distance function is also called Chebyshev distance and is defined as:

$$\boldsymbol{d_j} = \frac{|\boldsymbol{Z_j^*} - \boldsymbol{Z_j(x)}|}{|\boldsymbol{Z_j^*} - \boldsymbol{Z_{*j}}|} \tag{2}$$

Where $\boldsymbol{Z_j}(\boldsymbol{x})$ is the objetive function, $\boldsymbol{Z_j^*}$ is the utopian point which represents the ideal minimum solution, and $\boldsymbol{Z_{*j}}$ is the anti-ideal (nadir) point of the jth objetive. The normalised degrees $\boldsymbol{d_j}$ are expected to be between 0 and 1. If $\boldsymbol{d_j}$ is 0 it means that it has achieved its ideal solution. On the other hand, if $\boldsymbol{d_j}$ achieves 1, the objective function is showing the anti-ideal or nadir solution.

In practical terms, for compromise programming there is a need to know only the relative preferences of the decision maker for each objective. This process can be done by the weighted sum method. The method can transform multiple objectives into an aggregated objective function. The corresponding weight factors (p_{ith}) reflect the relative importance of each objective. This allows the decision maker to express the preferences by assigning a number between 0 and 1 to each objective. However, the sum of weight coefficient has to satisfy the following constraint:

$$\sum_{j=1}^{n} p_j = 1 \tag{3}$$

Therefore, the problem definition for compromise programming results in the following:

$$\alpha_j \geq \left(\frac{|\boldsymbol{Z_j^*} - \boldsymbol{Z_j(x)}|}{|\boldsymbol{Z_j^*} - \boldsymbol{Z_{*j}}|} \right) * (p_j) \tag{4}$$

where a minimisation of the Chebyshev distance α_j is sought.

5. ExRET-Opt subroutines verification

To ensure that ExRET-Opt is reliable, a validation or verification process is necessary. Due to lack of empirical exergy data, both an '*Inter-model Comparison*' using an existing tool and an '*Analytical Verification*' using various case studies found in the literature, are performed.

5.1 Inter-model verification (steady-state analysis)

The last version of the Annex 49 LowEx pre-design tool dates back in 2012. However, compared to ExRET-Opt, the LowEx tool lacks transient/dynamic calculation as it only relies on a steady-state energy balance analysis included in the spreadsheet. Additionally, it only considers heating and DHW as energy end-uses, lacking equations to calculate cooling and electric processes. Nevertheless, with the aim to test Module 3 within ExRET-Opt, steady-state calculations were performed. For the selection of the case study, the LowEx tool contains numerical examples of real pre-configured building cases. For this task '*The IEA SHC Task 25 Office Building*' is selected. The steady-state analysis considers a reference temperature of 0 °C and an internal temperature of 21 °C. The case studies input data can be seen in Table 2.

Table 2 Input data for simulation (Annex 49 pre-design tool example building)

Baseline characteristics - A/C Office	**Verification 1**
Case study	The IEA SHC Task25 Office Building
Number of floors	1
Floor space (m²)	929.27
Orientation (°)	0
Air tightness (ach)	0.6
Exterior Walls	U_{value}=0.35 (W/m²K)
Roof	U_{value}=0.17 (W/m²K)
Ground floor	U_{value}=0.35 (W/m²K)
Windows	U_{value}=1.10 (W/m²K)
Glazing ratio	32%
HVAC System	GSHP COP=3.5
Emission system	Underfloor Heating: 40/30°C
Heating Set Point (°C)	20.5
Cooling Set Point (°C)	--
*Occupancy (people)**	12.5
*Equipment (W/m²)**	1.36
*Lighting level (W/m²)**	2

5.1.1 Verification results

The comparison between the tools' outputs, is given in Table 3. Deviations between outputs are no larger than 5% with similar results in assessing energy supply chain exergy efficiency.

Table 3 Comparison of exergy rates results for inter-model verification

Subsystems	Annex 49 Pre-design tool	ExRET-Opt	Difference kW-(Deviation %)
Envelope (kW)	2.13	2.18	0.05 (+2.3%)
Room (kW)	2.47	2.47	0.00 (0.0%)
Emission (kW)	2.79	2.69	0.10 (-3.6%)
Distribution (kW)	4.51	4.37	0.14 (-3.1%)
Storage (kW)	4.51	4.37	0.14 (-3.1%)
Generation (kW)	11.51	11.77	0.26 (+2.3%)
Primary (kW)	30.75	30.00	0.75 (-2.4%)
Exergy efficiency ψ	6.95%	7.26%	--

Fig. 10 shows the exergy flow rate and the exergy loss rate by subsystems. As can be noted, no larger differences exist, and the model under steady-state conditions performs well.

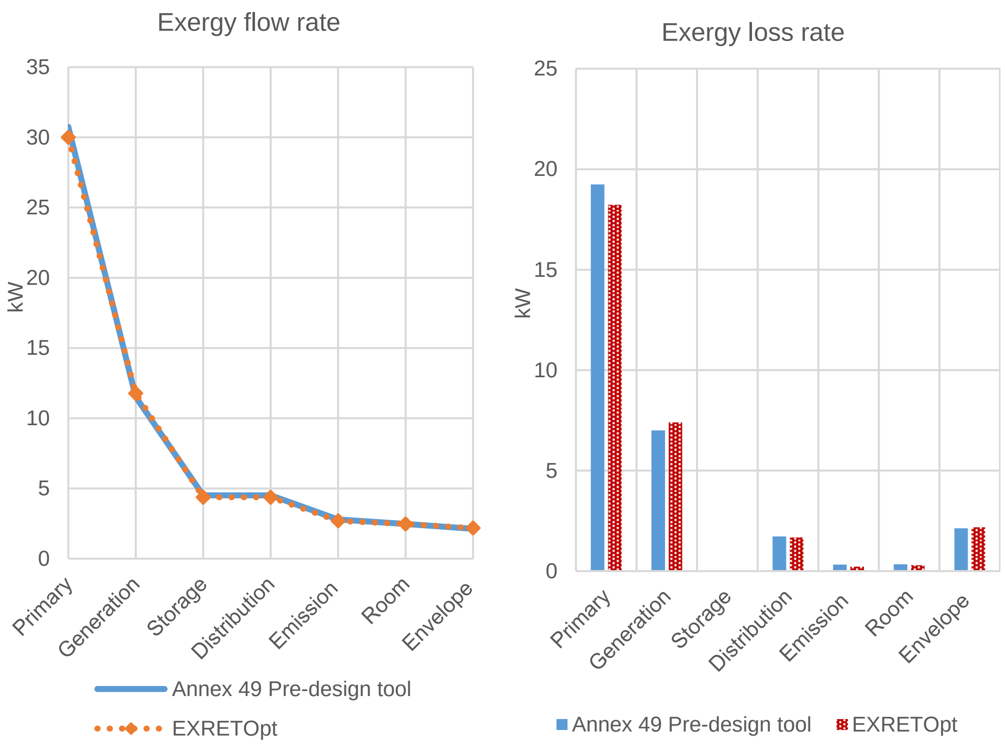

Fig. 10 Comparison of exergy flow rates and exergy loss rates by subsystems

By looking at the inter-model verification, it can be concluded that ExRET-Opt under steady-state calculation presents comprehensive results.

5.2 Analytical verification of subroutines

For the analytical verification, ExRET-Opt is compared against two numerical examples from the literature. The intention of this analysis is to verify the two 'Module 3' subroutines separately ('subroutine: *dynamicexergy'* and 'subroutine: *exergoeconomics')*. Although the research in dynamic building exergy and exergoeconomic analyses is limited, two highly cited articles can be relied on. Sakulpipatsin et al. [31] work can be used to verify the dynamic exergy analysis outputs, while Yücer and Hepbasli [55] work to verify exergoeconomic outputs.

5.2.1 *Dynamic exergy analysis verification and results*

Sakulpipatsin et al. [31] presented an exploratory work showing the application of dynamic exergy analysis in a single-zone model. These dynamic calculations were implemented in TRNSYS dynamic simulation tool. The case study building is a cubic-box with a net floor area of 300 m^2 spread along 3 stories. The heating system is based on district heating supplying hot water at 90 °C. The cooling system is based on a small-scale chiller with a COP of 1.5. Both systems supply the thermal energy to a low-temperature heating/high-temperature cooling panels. For the reference temperature, the De Bilt, Netherlands weather file is used as it was the reference weather file used in the original research. The full input data of the building and its HVAC system can be seen in Table 4.

Table 4 Input data for analytical verification of subroutine: *dynamicexergy* within ExRET-Opt

Baseline characteristics A/C Office	Verification
Case study	Office building
Location	De Bilt, Netherlands
Number of floors	3
Floor space (m^2)	300
Orientation (°)	0
Air tightness (ach)	0.6
Natural ventilation rate (m3/h)/m3	4
Exterior Walls	U-value=0.511 (W/m^2K)
Roof	U-value=0.316 (W/m^2K)
Ground floor	U-value=0.040 (W/m^2K)
Windows	U-value=1.300 (W/m^2K)
Glazing ratio	42.5% (south façade only)
HVAC System	Heating: District Heating, T: 90 Cooling: Small Chiller COP: 1.5 (In both cases, distribution pipes have a temperature drop of 10 °C)
Emission system	Low temperature Heating: 35/28°C High Temperature Cooling: 10/23 °C
Heating Set Point (°C)	20
Cooling Set Point (°C)	24
*Occupancy (people)**	30 (75 W per person)
*Equipment (W/m^2)**	23
*Lighting level (W/m^2)**	1.33

Table 5 compares two groups of data (heating and cooling) between the research data and ExRET-Opt outputs. The results show the exergy demand at each part of the supply chain, considering auxiliary energy for the HVAC system components. The corresponding differences in absolute value and in percentage are also shown. Results show that ExRET-Opt is capable of accurately predicting the heating exergy performance of the system. In the cooling case, larger deviations' percentage can be noted, mainly due to lower values, where small absolute value discrepancies can represent larger deviations. If compared to the heating case, the absolute values for cooling are much lower. However, since different weather files are used, the outputs seem reasonable. Nevertheless, efficiency values are rather similar.

Table 5 Comparison of annual exergy use results for analytical verification of ExRET-Opt

	Sakulpipatsin et al. [31]	**ExRET-Opt**	**Difference - (Deviation %)**
Heating case Subsystems			
Building (kWh/m^2-y)	5.66	4.51	1.15 (-20.31%)
Emission (kWh/m^2-y)	16.17	13.93	2.24 (-16.6%)
Distribution (kWh/m^2-y)	19.57	16.46	3.11 (-15.9%)
Primary Generation (kWh/m^2-y)	33.03	33.78	0.75 (+1.14%)
Exergy efficiency Ψ	17.13%	13.35%	--
Cooling case Subsystems			
Building (kWh/m^2-y)	0.17	0.37	0.20 (+117.6%)
Emission (kWh/m^2-y)	0.25	0.80	0.55 (+220.0%)
Distribution (kWh/m^2-y)	0.33	0.88	0.55 (+166.6%)
Primary Generation (kWh/m^2-y)	2.63	4.39	1.76 (+66.9%)
Exergy efficiency Ψ	6.46%	5.95%	--

Considering that the analysis is done at an hourly rate, the 'subroutine: *dynamicexergy'* seems to provide reliable results. However, the cooling calculations need further testing.

5.2.2 Exergoeconomics verification and results

In existing relevant literature, no comprehensive example of a dynamic exergy analysis combined with an exergoeconomic analysis applied to a building exists. However, Yücer and Hepbasli [55] performed a steady-state exergy and exergoeconomic analysis of a building's heating system, based on the SPECO method. The limitation of this research is that the exergy outputs are presented for just one temperature, neglecting the dynamism of an actual reference environment. For the case study, a house accommodation of 650 m² is considered. The reference environment is taken as 0 °C, with an internal temperature of 21 °C. The HVAC system is composed of a steam boiler, using fuel oil that provides thermal energy to panel radiators to finally heat the room. Solar and internal heat gains have been neglected. The characteristics of the case study can be seen in Table 6.

Table 6 Input data for analytical verification of subroutine: exergoeconomics within ExRET-Opt

Baseline characteristics A/C Office	Verification
Case study	House accommodation building
Location	Izmir, Turkey
Number of floors	3
Floor space (m²)	650
Orientation (°)	0
Air tightness (ach)	1.0
Natural ventilation rate (m3/h)/m3	--
Exterior Walls	U_{value}=0.96 (W/m²K)
Roof	U_{value}=0.43 (W/m²K)
Ground floor	U_{value}=0.80 (W/m²K)
Windows	--
Glazing ratio	--
HVAC System	Heating: Oil Boiler, T: 110 °C (Distribution pipes have a temperature drop < 10 °C)
Emission system	Radiator panels Heating: 35/28°C
Heating Set Point (°C)	21
Cooling Set Point (°C)	--
*Occupancy (people)**	--
*Equipment (W/m²)**	--
*Lighting level (W/m²)**	--

However, another limitation exists for the exergoeconomic analysis, as the authors have reduced the subsystems' analysis from seven to just three: generation, distribution, and emission subsystems. Since the capital cost of the subsystem is essential for this analysis, this is provided in Table 7.

Table 7 Components capital cost of the building HVAC system

Subsystems	Capital cost ($)[2]
Distribution pipes	3,278
Radiator panels	5,728
Steam boiler	13,810
Envelope	3,959

The exergy price of the fuel is fundamental for exergoeconomic analysis as is it the product price entering the analysed stream. Only the heating mode is analysed, where fuel oil is

[2] Monetary values (USD) given as per original source

utilised. As the energy quality for oil is set at 1.0, both the energy price and exergy price are considered similar (0.096 $/kWh).

Table summarises the results for this verification. First, a comparison of the steady-state exergy analysis is done to ensure that exergy values are within acceptable range. Some deviations are found, with the greatest at the room air subsystem (31.9%). However, as the deviations for the other subsystems are lower and the overall exergy efficiency of the whole system is similar, the obtained results seem acceptable.

Table 8 Comparison of exergy rates results for subroutine: exergoeconomics verification

Subsystems	Yücer and Hepbasli [55]	ExRET-Opt Exergy analysis	Difference (Deviation %)
Envelope (kW)	3.78	3.11	0.67 (-17.7%)
Room (kW)	11.93	8.13	3.80 (-31.9%)
Emission (kW)	12.61	13.20	0.61 (-4.6%)
Distribution (kW)	17.15	18.09	0.94 (+5.5%)
Generation (kW)	82.38	94.98	-12.60 (+15.3%)
Primary (kW)	107.09	101.44	-5.65 (-5.3%)
Exergy efficiency Ψ	3.53%	3.06%	--

Table shows the verification of the exergoeconomic outputs for the reduced system analysis. Cost of fuels and products at each stage of the energy supply chain presented a similar increase trend. However due the simplicity of the steady-state approach by Yücer and Hepbasli [55], a great part of exergy destruction cost is not accounted correctly. On the other hand, ExRET-Opt calculates the exergy cost formation throughout the whole thermal energy supply chain.

Table 9 Exergoeconomic comparison between research and ExRET-Opt

Subsystems	Yücer and Hepbasli [55] Exergoeconomic analysis			ExRET-Opt Exergoeconomic analysis			Difference (Deviation %)		
	C, product $/kWh	Z $/h	C, fuel $/kWh	C, product $/kWh	Z $/h	C, fuel $/kWh	C, product $/kWh	Z $/h	C, fuel $/kWh
Generation	0.096	0.46	0.628	0.096	0.44	0.327	0.00 (0.0%)	0.02 (-4.3%)	0.301 (-48.1%)
Distribution	0.628	0.07	0.861	0.327	0.07	0.726	0.301 (-48.1%)	0.00 (0.0%)	0.135 (-15.7%)
Emission	0.861	0.17	0.925	0.726	0.18	0.812	0.135 (-15.7%)	.01 (+5.9%)	.0113 (-12.2%)

Fig. 11 illustrates the stream cost increase comparison. The exergy cost formation increase is due to the system inefficiencies in the energy supply system with high volumes of exergy destructions. At each stage, an amount of economic value is added to the energy stream when it passes the energy supply chain.

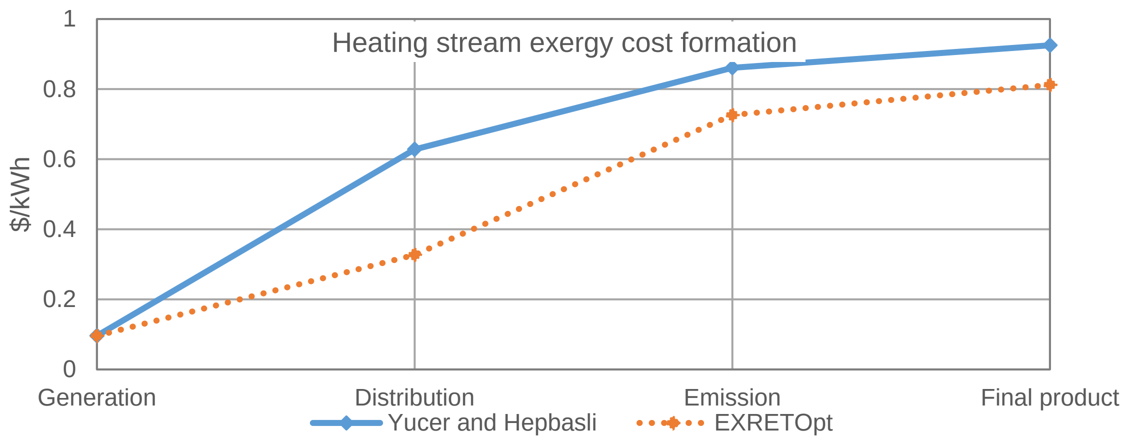

Fig. 11 Exergoeconomic cost increase of the stream

Although the graph shows a similar behaviour, the deviations can be related to several factors. One is that ExRET-Opt performs the calculation for a supply chain composed of 7 subsystems, so exergy formation is more detailed and considers inefficiencies of different type of equipment. Another factor, is that the author does not mention the number of hours that the equipment is working, which affects the capital cost rate ($\dot{Z}$) and thus affects the exergy cost formation of the stream. However, final cost deviation was only found at 12.2%.

6. ExRET-Opt application

6.1 Case study and baseline values

To demonstrate ExRET-Opt capabilities, this has been applied to recently retrofitted primary school building (1900 m²) located in London, UK. The simulation model consists of a fourteen-thermal zone building. The largest proportion of the floor area is occupied by classrooms, staff offices, laboratories, and the main hall. Other minor zones include corridors, bathrooms, and other common rooms. Heating is provided by means of conventional gas boiler and high temperature radiators (80°C/60°C) with no heat recovery system. As no artificial cooling system is regarded, natural ventilation is considered during summer months. A schematic layout of the building energy system is illustrated in Fig. 12. Buildings thermal properties as well as energy benchmark indices are presented in Table 10. Properties such as occupancy schedules and inputs as well as environmental values are taken from the UK NCM [74] and Bull et al. [75].

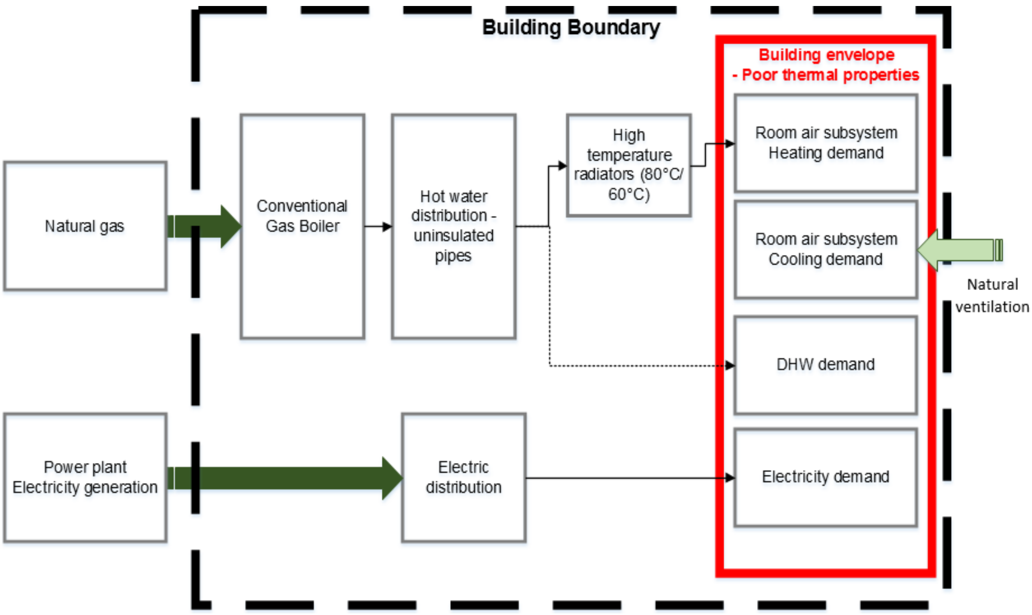

Fig. 12 Schematic layout of the energy system for the Primary School base case

Table 10 Primary school baseline building model characteristics

Baseline characteristics	Primary School
Year of construction	1960s
Number of floors	2
Floor space (m^2)	1,990
Orientation (°)[+]	227
Air tightness (ach)[+]	1.0
Exterior Walls[+]	Cavity Wall-Brick walls 100 mm brick with 25mm air gap U_{value}=1.66 (W/m²K)
Roof[+]	200mm concrete block U_{value}=3.12 (W/m²K)
Ground floor[+]	150mm concrete slab U_{value}=1.31 (W/m²K)
Windows[+]	Single-pane clear (5mm thick) U_{value}=5.84 (W/m²K)
Glazing ratio	28%
HVAC System[+]	Gas-fired boiler 515 kW η = 82% No cooling system
Emission system	Heating: HT Radiators 90/70°C Cooling: Natural ventilation
Heating Set Point (°C)[+]	19.3
Cooling Set Point (°C)[+]	--
Occupancy (people/m^2)[+*]	2.1
Equipment (W/m^2)[*+]	2.0
Lighting level (W/m^2)[*+]	12.2
EUI electricity (kWh/m^2-y)	45.6
EUI gas (kWh/m^2-y)	142.3
Annual energy bill (£/y)	19,449
Thermal discomfort (hours)	1,443
CO_2 emissions (Tonnes)	214.8

By end-use, heating represents 58.1% of the total energy demand, meaning that the 515 kW gas fired boiler consumes 781.7 GJ/year of natural gas. This is followed by 238.2 GJ/year for DHW (17.7%) and 59.0 GJ/year of electricity for interior lighting (13.7%). Fans, mainly used for mechanical cooling and extraction also have an intensive use, demanding 66.1 GJ/year, representing 4.9% of the total energy demand.

The outputs from the economic analysis deliver an annual energy bill of £19,449.3 for the building, where £10,949.6 is needed to cover electricity demand and £8,499.6 for natural gas. In addition, the LCC (over 50 years) obtained is found at £500,425 (£251.5/m²).

6.1.1 Primary School baseline exergy flows and exergoeconomic values

The building requires a total primary exergy input of 1,915.9 GJ/year (264.4 kWh/m²-year). By product type, electric-based equipment requires the largest share of 861.9 GJ (45%), followed by heating with 807.7 GJ (42.2%) and DHW with 246.3 GJ (12.8%). Fig. 13 shows the annual exergy flows for the three products analysed. Exergy flow diagrams give a first insight in the exergy behaviour inside the different building energy systems.

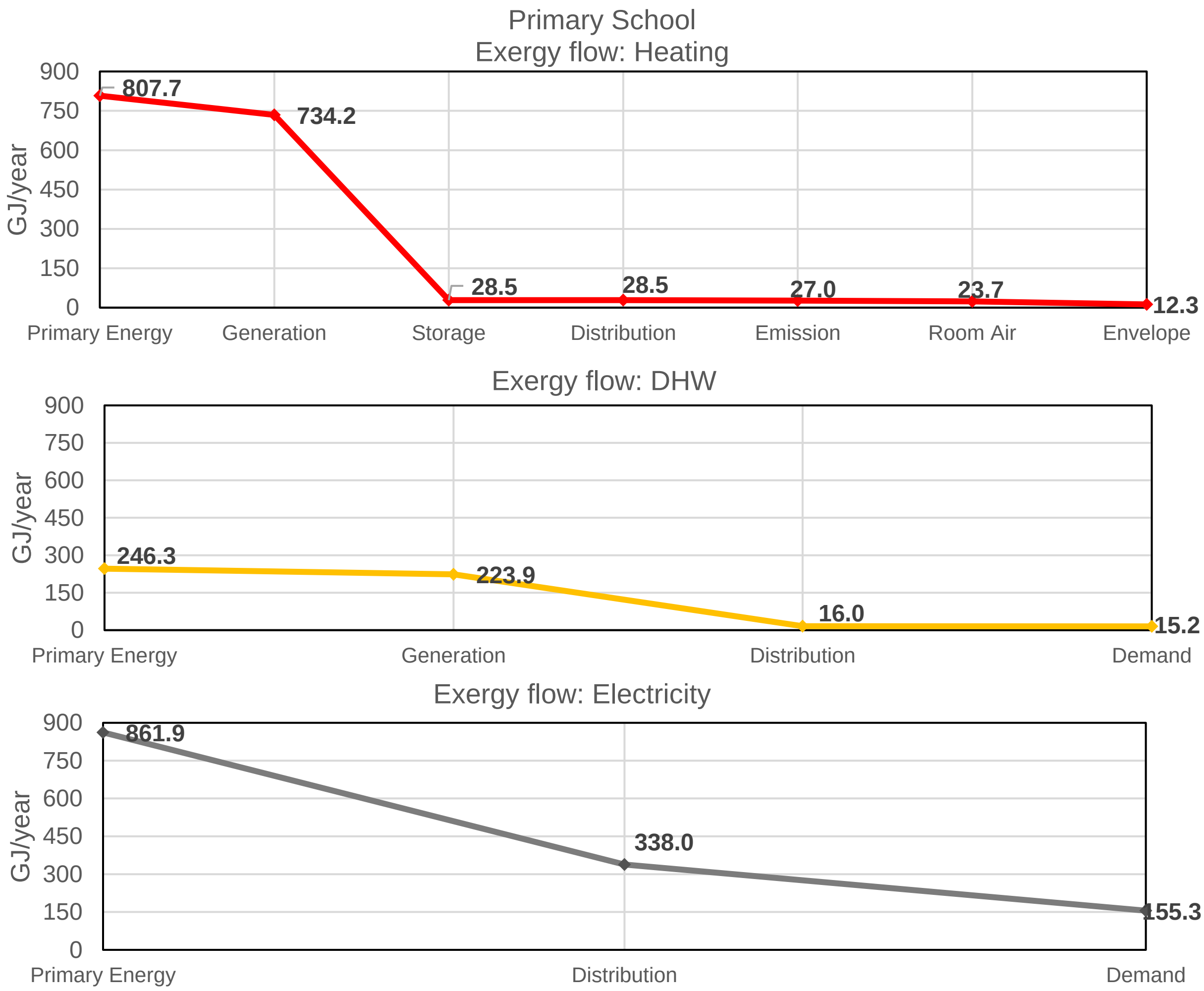

Fig. 13 Exergy flows by product type. Primary School

Fig. 14 illustrates the building heating product cost formation throughout the energy supply chain, showing that the heating product at the thermal zone increases from £0.03/kWh (gas price) to £1.79/kWh, with a total relative cost difference r_k of 58.66.

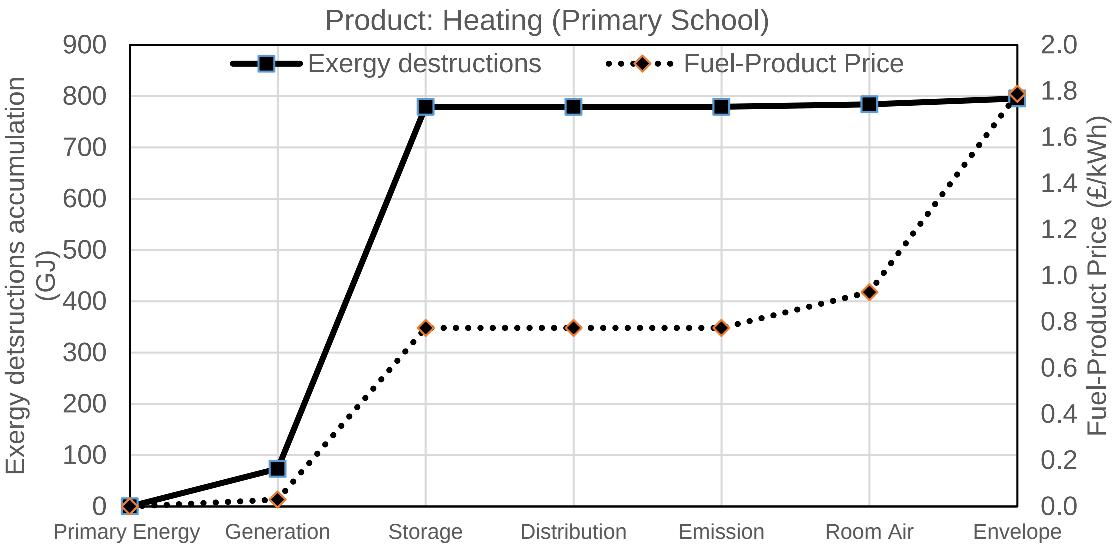

Fig. 14 Exergy destruction accumulation vs product cost formation for the heating stream. Primary School

Until now, as no retrofit strategy has been implemented, no capital cost and revenue can be calculated ($\dot{Z}_{sys} = 0$, $\dot{R} = 0$). Therefore, the $Exec_{CB,baseline}$ or $\dot{C}_{D,sys}$ has a value of £2.72/h (£17,672.9/year). By products, exergy destructions cost from heating processes represents 67%, electric appliances 26%, and DHW 7%. The baseline exergy and exergoeconomic values can be seen in Table 11.

Table 11 Baseline exergy and exergoeconomic values

Baseline characteristics	Primary School
Exergy input (fuel) (GJ)	1915.9
Exergy demand (product) (GJ)	182.8
Exergy destructions (GJ)	1733.1
Exergy efficiency HVAC	1.5%
Exergy efficiency DHW	6.2%
Exergy efficiency Electric equip.	18.0%
Exergy efficiency Building	9.5%
Exergy cost fuel-prod HEAT (£/kWh) {r_k}	0.03—1.79 {58.66}
Exergy cost fuel-prod COLD (£/kWh) {r_k}	----- {---}
Exergy cost fuel-prod DHW (£/kWh) {r_k}	0.03—0.44 {13.66}
Exergy cost fuel-prod Elec (£/kWh) {r_k}	0.12—0.26 {1.16}
D (£/h) Exergy destructions cost (energy bill £; %D from energy bill}	2.72 {17,672.9; 90.8%}
Z (£/h) Capital cost	0
Exergoeconomic factor f_k (%)	1
Exergoeconomic cost-benefit (£/h)	**2.72**

6.2 Optimisation

6.2.1 Algorithm settings

a) Objective functions

As mentioned, an energy optimisation problem requires at least two conflicting problems. In this study three objectives that have to be satisfied simultaneously are going to be investigated. These are the minimisation of overall exergy destructions, reduction of occupant thermal discomfort, and maximisation of project's Net Present Value:

I. Building annual exergy destructions (kWh/m^2-year):

$$Z_1(x)\, min = \; Ex_{dest,bui} \; = \sum Ex_{prim}(t_k) - \sum Ex_{dem,bui}\,(t_k) \quad (5)$$

II. Occupant discomfort hours:

$$Z_2(x) min = \; \left(PMV \,\middle|\, > 0.5\right) \quad (6)$$

III. Net Present Value$_{50\ years}$ (£):

$$Z_3(x) max = \; NPV_{50 years} \; = -TCI + \left(\sum_{n=1}^{N} \frac{R}{(1+i)^n}\right) + \frac{SV_N}{(1+i)^N} \quad (7)$$

However, for simplification and to encode a purely minimisation problem, the NPV is set as negative (although the results will be presented as normal positive outputs). Therefore:

$$Z_3(x) min = \; -NPV_{50 years} \; = -\left\{-TCI + \left(\sum_{n=1}^{N} \frac{R}{(1+i)^n}\right) + \frac{SV_N}{(1+i)^N}\right\} \quad (8)$$

b) Constraints

Furthermore, it was chosen to subject the optimisation problem to three constraints. First, as a pre-established budget is one of the most common typical limitations in real practice, it was decided to use the initial total capital investment as a constraint. From a previous research [58], a deep retrofit design for this exact same building was suggested with an investment of £734,968.1; therefore, this budget was taken as an economic constraint. In this instance, the aim is to test ExRET-Opt to deliver cheaper solutions with better energetic, exergetic, economic, and thermal comfort performance. Additionally, DPB is also considered as a constraint, sought for solutions with a DPB of 50 years or less, giving positive NPV values. Finally, a third constraint is the maximum baseline discomfort hours, subjecting the model not to worsen the initial baseline conditions (1,443 hours). Hence, the complete optimisation problems can be formulated as follows:

Given a ten-dimensional decision variable vector $x = \{X^{\mathrm{HVAC}}, X^{\mathrm{wall}}, X^{\mathrm{roof}}, X^{\mathrm{ground}}, X^{\mathrm{seal}}, X^{\mathrm{glaz}}, X^{\mathrm{light}}, X^{\mathrm{PV}}, X^{\mathrm{wind}}, X^{\mathrm{heat}}\}$, in the solution space X, find the vector(s) x^* that:

Minimise: $Z(x^*) = \{Z_1(\mathrm{x}*), Z_2(\mathrm{x}*), Z_3(\mathrm{x}*)\}$

Subject to follow inequality constraints: $\begin{cases} TCI \le £734{,}968 \\ DPB \le 50\ years \\ Discomfort \ \le 1{,}443\ hrs \end{cases}$ {constraints}

c) NSGA-II parameters

As GA requires a large population size to efficiently work to define the Pareto front within the entire search space, Table 12 shows the selected algorithm parameters.

Table 12 Algorithm parameters and stopping criteria for optimisation with GA

Parameters	
Encoding scheme	Integer encoding (discretisation)
Population type	Double-Vector
Population size	100
Crossover Rate	100%
Mutation Rate	20%
Selection process	Stochastic – fitness influenced
Tournament Selection	2
Elitism size	Pareto optimal solutions
Stopping criteria	
Max Generations	100
Time limit (s)	10^6
Fitness limit	10^{-6}

6.3 Results optimisation

6.3.1 Dual-objective analysis

In this section, the performance of the system can be presented as a trade-off between the pairs of objectives to easily illustrate Pareto solutions. This represents an analysis of the three sets of dual objectives: *1) Exergy destructions – Comfort, 2) Exergy Destruction – NPV, and 3) Comfort – NPV*. All simulated solutions, the solutions constrained by the selected criteria, the baseline case, and the Pareto front are represented in the following graphs. Each solution in the Pareto front has associated different BER strategies.

Fig. 15 illustrates the simultaneous minimisation of exergy destructions and discomfort hours, localising the constraint solutions and the Pareto front, formed by eleven designs. Models with better outputs in the objectives that are not part of the Pareto front are due to the established constraints, either related to thermal comfort, capital investment, or cost-benefit. When analysing the Pareto front, the most common HVAC systems are H10: Biomass boiler with CAV system and H28: Biomass Boiler with wall heating, both with a frequency of 27.3%. For insulation, no measures with exact technology and thickness repeat; however, the most common technology is EPS for the wall, Polyurethane and EPS for the roof, and polyurethane for the ground floor. In respect to the infiltration rate, 0.7 *ach* is the most common value. For active systems, the T8 LED lighting system, with no PV panels and wind turbines are the most frequent variables. The minimum value for exergy destructions is achieved by the system H28, while the minimum value for discomfort by the H10. The whole description of the BER designs for both optimised extremes can be seen in the graph. Also, the BER design that represents the model closer to the 'utopia point' is presented. The utopia point is represented by a theoretical solution that has both optimised values.

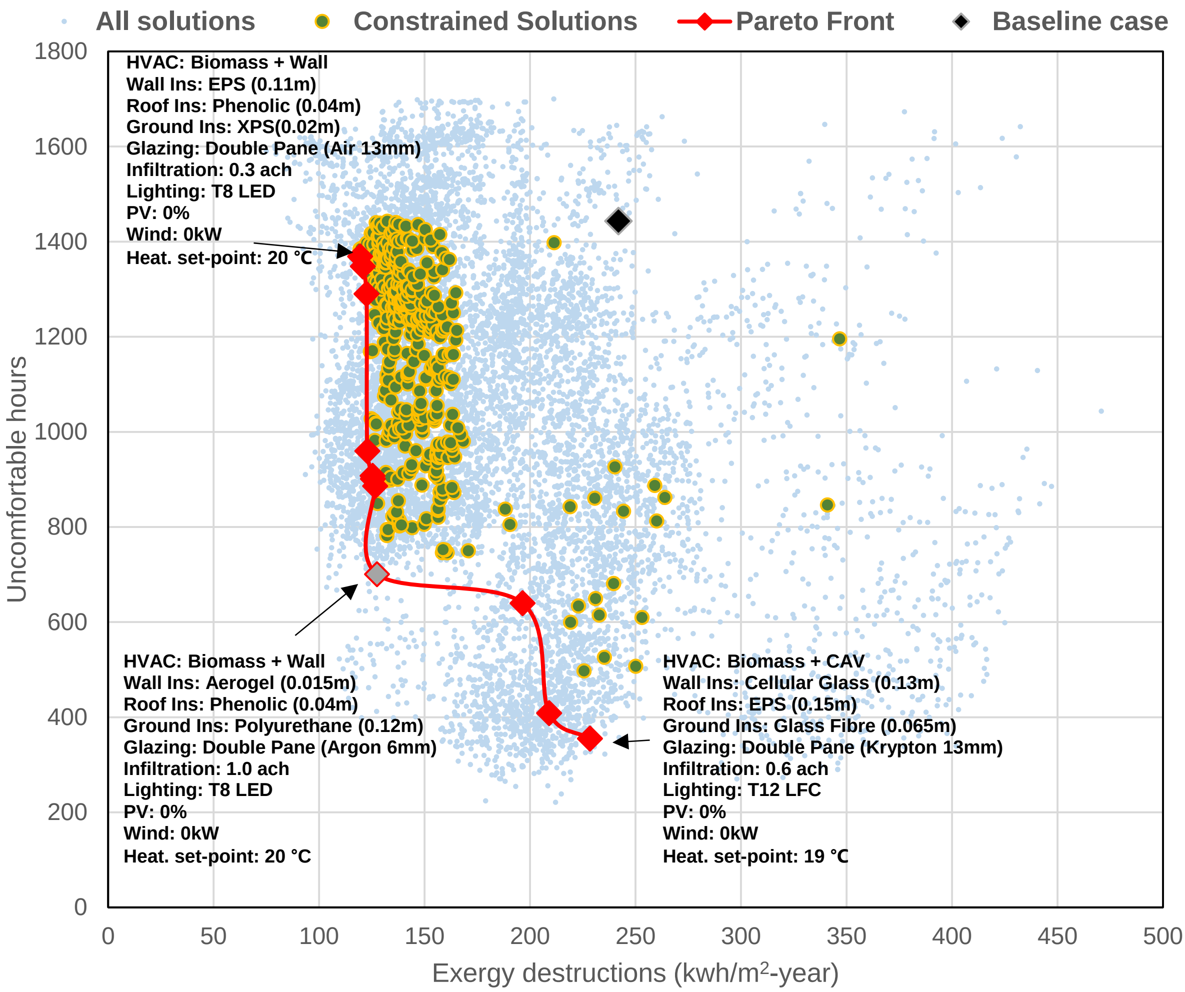

Fig. 15 Optimisation results and Pareto front (Exergy destructions - Comfort) for the Primary School

Fig. 16 illustrates the simultaneous minimisation of exergy destructions and maximisation of NPV. In this case, the Pareto front is formed by nine designs. The most frequent HVAC design is H31: microCHP with a CAV system, presented in eight of the nine cases. The only other system is H28: Biomass boiler and Wall heating. For the wall insulation, the most frequent technologies are EPS and glass fibre, while for both roof and ground is EPS. The most common infiltration rate is 0.4 *ach*, with a frequency of 44.4%, while the most frequent glazing system (33.3%) is double glazing with 6 mm gap of Krypton. For the lighting system it is T5 LFC, and again no renewable systems are common, where just one of the models includes a 20 kW wind turbine.

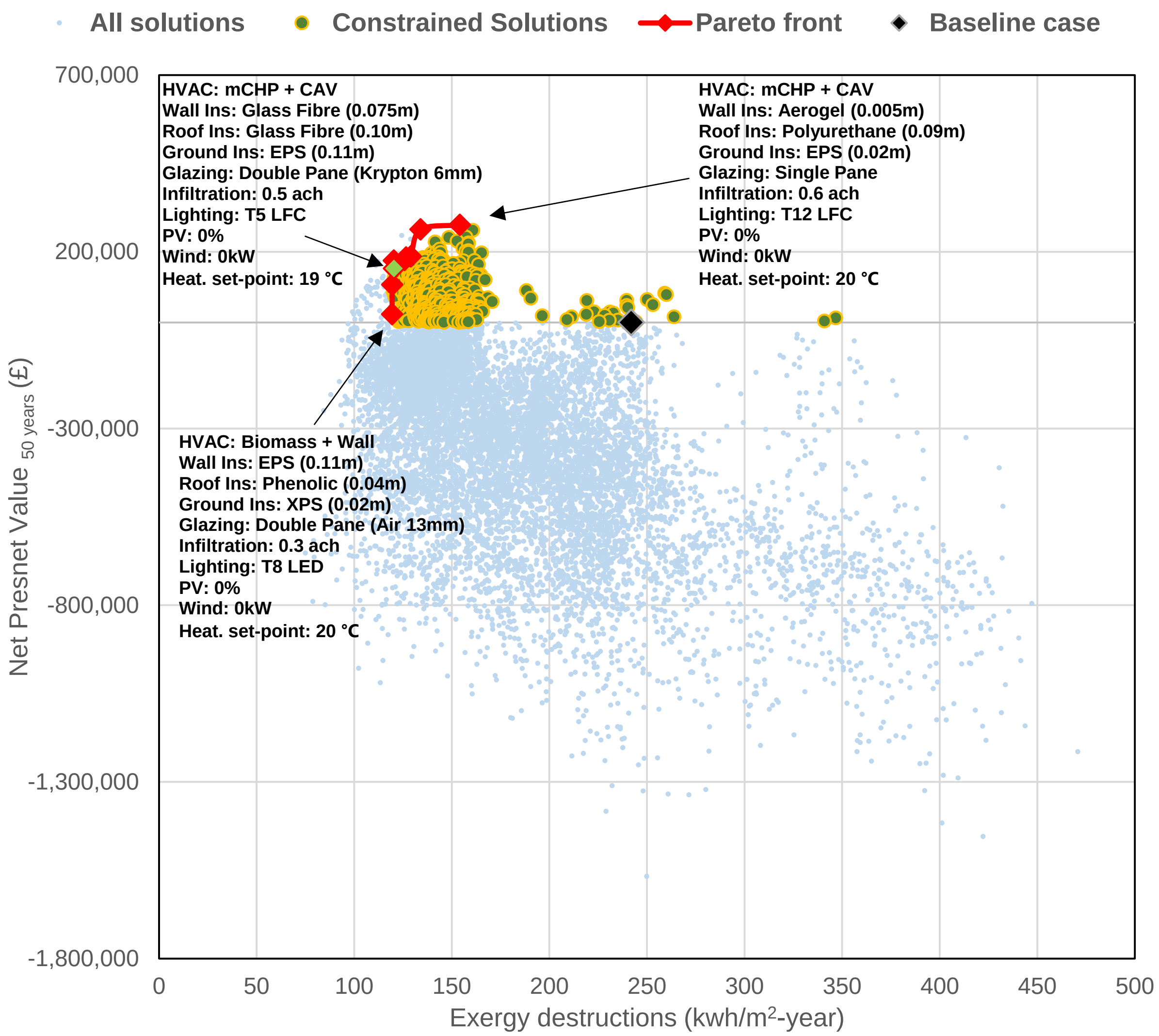

Fig. 16 Optimisation results and Pareto front (Exergy destructions - NPV) for the Primary School

The results for the dual optimisation of thermal comfort and NPV are illustrated in Fig. 17. The Pareto front is formed by thirteen solutions. The most common HVAC system is H28: Biomass boiler and wall heating with a recurrence of 46.2%. The most common insulation measures are cellular glass and cork board for the walls, EPS for the roof, and polyurethane for the floor. The infiltration rate that dominates the optimal solutions is 0.8 *ach*, with no retrofit in the glazing system. Regarding active systems, the baseline's T12 LFC is the most common solution with no installation of PV panels and wind turbines.

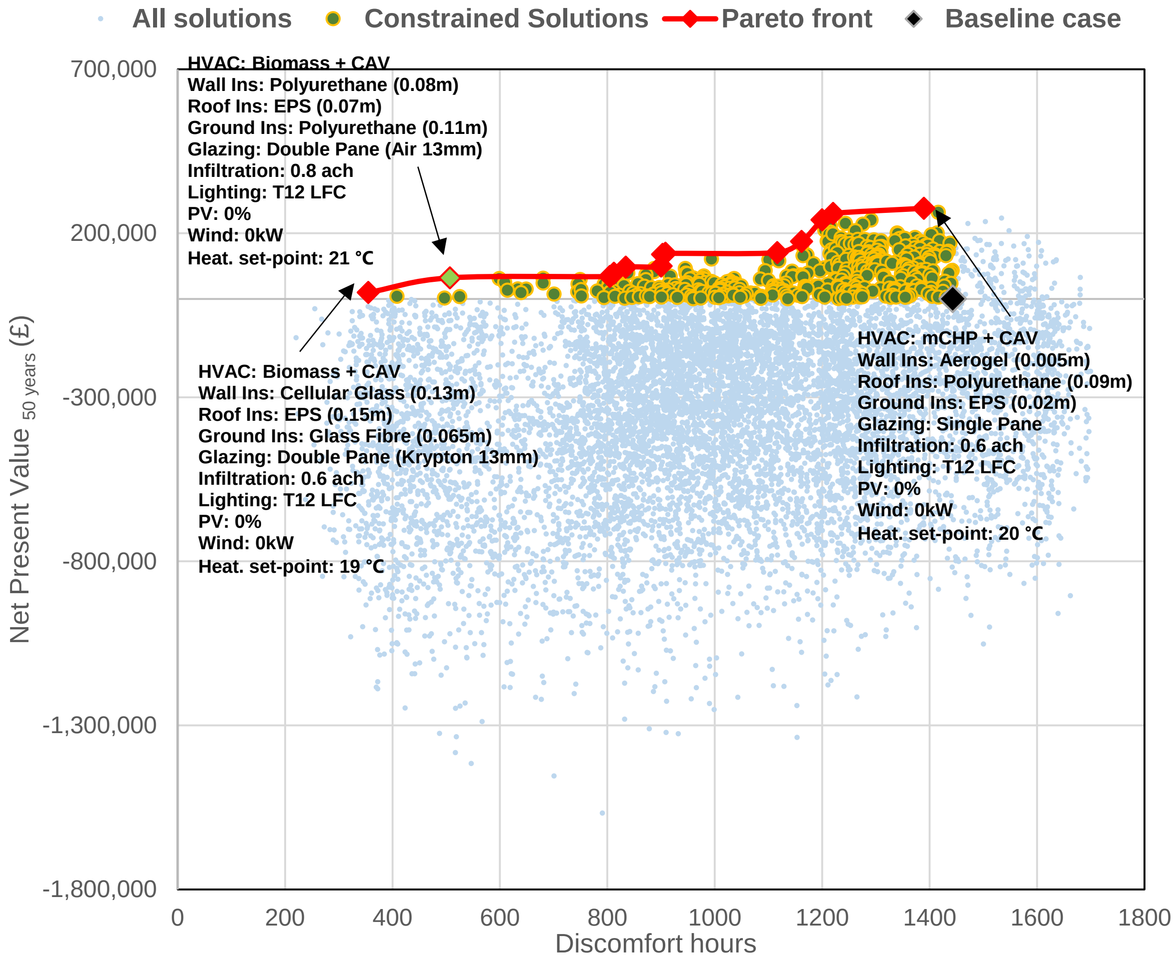

Fig. 17 Optimisation results and Pareto front (Comfort - NPV) for the Primary School

6.3.2 Triple-objective analysis

The constrained solutions' space consists of 417 models, of which the Pareto surface is composed of only 70 possible solutions. Given the constraints, the Pareto results suggest that the optimisation study found more models oriented to minimise exergy destructions and maximise NPV, while struggling to optimise the thermal comfort objective. This is also complemented by the fact that the majority of optimal solutions present high values of infiltration levels (0.5 < x <1.0 ach). This might be the case for obtaining average improvement in occupant thermal comfort. Nevertheless, the Pareto front also obtained models with good thermal comfort performance, with discomfort values of 400 hours or less annually. Regarding the HVAC system, H31: mCHP with CAV system is presented in the majority of optimal solutions. On the other hand, the optimisation suggests not to retrofit the glazing systems due to its high capital investment costs. In respect to insulation, Polyurethane is found to be the most frequent technology among all three parts of the envelope. The most common insulation thicknesses are found to be 5 cm, 1cm, and 2 cm for wall, roof, and ground respectively. Fig. 18 shows the frequency distribution of the main BER solutions in the Pareto front.

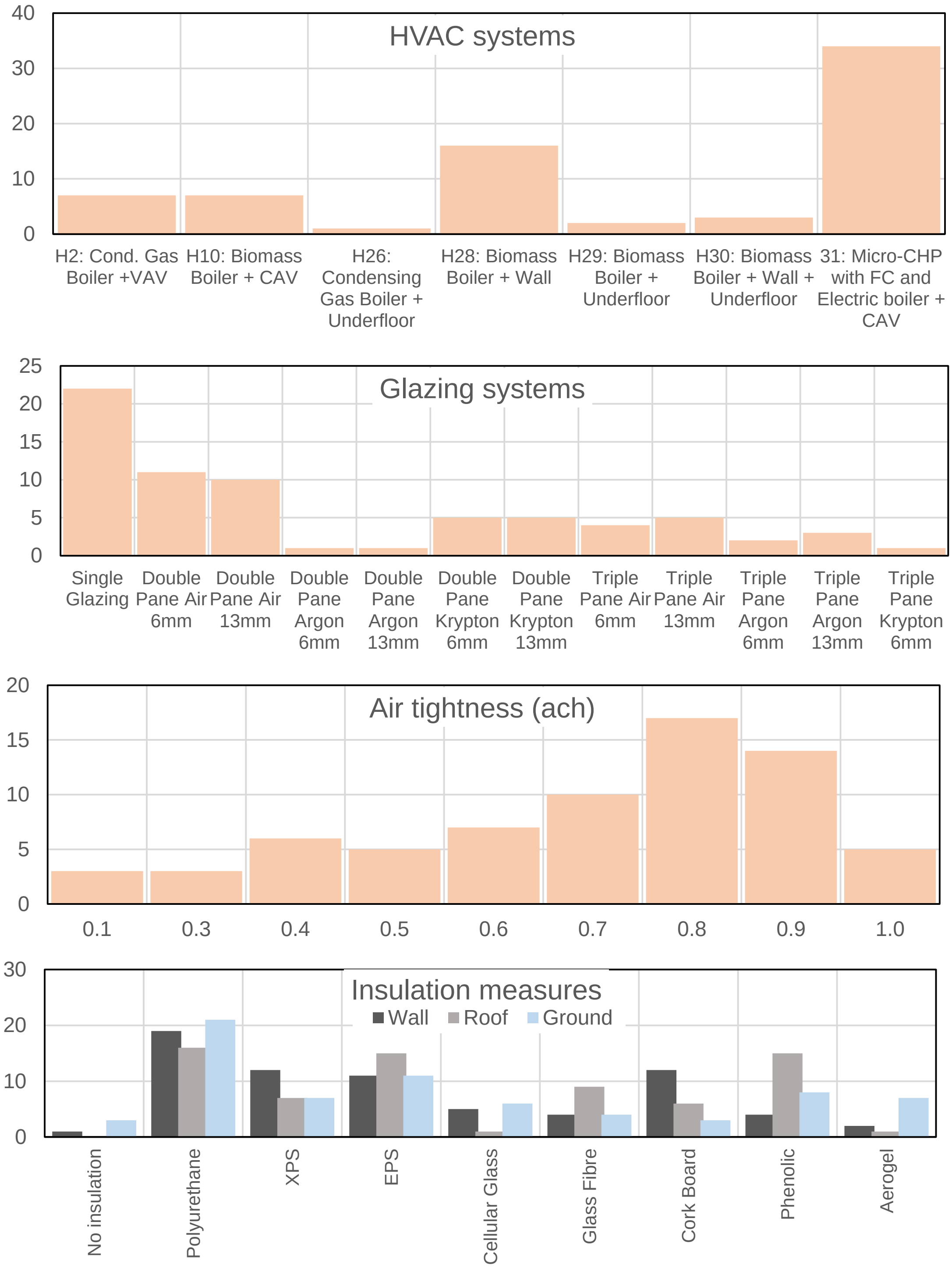

Fig. 18 Frequency distribution graphs of main retrofit variables from the Pareto front for the Primary School case study

Other design variables that are not illustrated and dominate the Pareto front are T12 LFC for the lighting system, the implementation of a 20 kW wind turbine, lack of installation of PV roof panels, and a heating set-point of 18 °C. This set-point variable also impacts the poor improvement in thermal comfort.

6.3.3 Algorithm behaviour - Convergence study

For both cases, the convergence metrics were computed for every generation. Fig. 19 illustrates the evolution of the three objective functions corresponding to each generation and its convergence with an allowance of one hundred generations. The results demonstrate that exergy destructions converged after the nineteenth generation (119.4 kWh/m^2-year), discomfort hours converged after the fiftieth (355 hours), and NPV after the twenty-fifth generation (£276,182). As it can be seen, the minimum value for exergy destructions found in the first generation (129.8 kWh/m^2-year) is similar to the one found in the last generations, meaning that the algorithm selected a 'strong' and 'healthy individual' (building model) from the first generation. However, due to the model's strict constraints, larger number of generations are required for the discomfort hours to converge within an acceptable value.

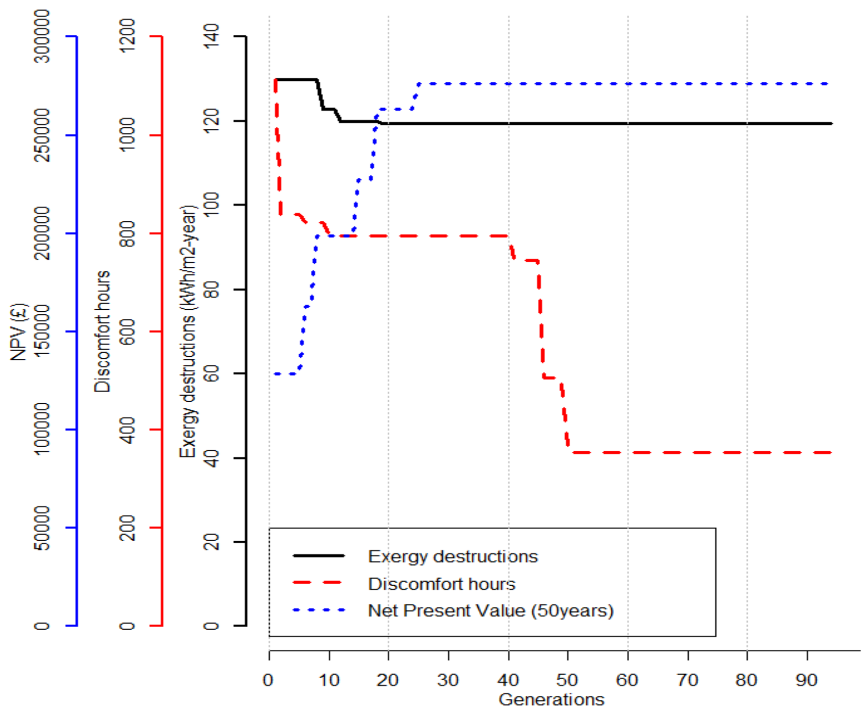

Fig. 19 Convergence of Primary School optimisation procedure for the three objective functions

6.4 Multiple-criteria decision analysis (compromise programming)

In order to tackle the multi-objective optimisation procedure within ExRET-Opt, the MCDM module is used. In compromise programming, firstly, the non-dominated set is defined with respect to the ideal (Utopian - Z^*) and anti-ideal (Nadir - Z_*) points, which represent the optimisation and anti-optimisation of each objective individually. For this study, the process can be written as follows:

$$\alpha_{exergy\_dest} \geq \left(\frac{\left| Z_{exergy\_dest}(x) - Z^*_{exergy\_dest} \right|}{\left| Z^*_{exergy\_dest} - Z_{*exergy\_dest} \right|} \right) * \left(p_{exergy\_dest} \right) \quad (9)$$

$$\alpha_{discomfort} \geq \left(\frac{\left| Z_{discomfort}(x) - Z^*_{discomfort} \right|}{\left| Z^*_{discomfort} - Z_{*discomfort} \right|} \right) * \left(p_{discomfort} \right) \quad (10)$$

$$\alpha_{NPV} \geq \left(\frac{\left| Z^*_{NPV} - Z_{NPV}(x) \right|}{\left| Z^*_{NPV} - Z_{*NPV} \right|} \right) * \left(p_{NPV} \right) \quad (11)$$

For the application of compromise programming, the weighting procedure by scanning different combinations for the three objectives is subject to the following constraint:

$$\sum_{j=1}^{n} p_j = p_{exergy\_dest} + p_{discomfort} + p_{NPV} = 1 \quad (12)$$

Finally, as an individual distance (α_j) is obtained for each objective, these are added up for every solution:

$$\alpha_{cheb} = \sum_{j=1}^{n} \alpha_j = \alpha_{exergy\_dest} + \alpha_{discomfort} + \alpha_{NPV} \geq 0 \quad (13)$$

The method then scans all the feasible sets and minimises the deviation from the ideal point, obtaining the minimum Chebyshev distance ([min]α_{cheb}):

$$[min]\alpha_{cheb} = min \sum_{j=1}^{n} \alpha_j \quad (14)$$

For the case study, the entire range of defined criteria and different weights of coefficient values is summarised in Appendix B. The table shows the best solution for each weighting design showing the BER retrofit parameters code (Appendix A) along the obtained results for each objective function. Having this type of information gives the decision maker the flexibility and possibility of a straightforward BER design change, if new insights arise as a result of the objectives' priorities adjustment. From a detailed analysis of the outputs, it is found that only nine solutions are considered by the MCDM, as similar BER design repeats in different weighting coefficients (Fig. 20).

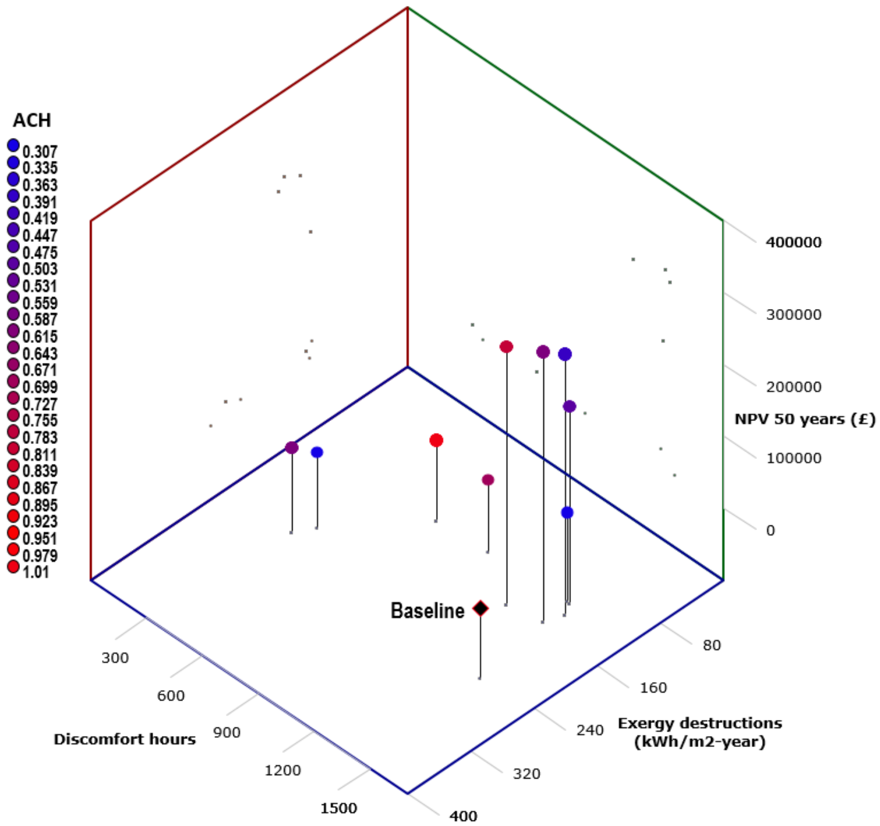

Fig. 20 Primary School optimal solutions found by Compromise Programming MCDM method

Fig. 21 shows the compromise solutions for different weights for all pairs of objective functions combinations, demonstrating how the objective functions' outputs change with respect to the coefficient weight. These graphs show the competitive nature of all three objectives. For example, as a result of demanding more exergy to cover internal thermal conditions, an increase in exergy destructions leads to a decrease in occupant thermal discomfort. However, meeting at p_{exergy}=0.4 and $p_{discomfort}$=0.6 good solutions for both objectives can be obtained. When comparing NPV and exergy destructions, it demonstrates that projects with higher NPV merely increase exergy destructions, meaning that a compromise in building exergy efficiency could lead to a more profitable project. Finally, a less profitable project (low NPV) is required to obtain good internal conditions as a result of two reasons: the necessity of more energy leading to a larger expenditure and/or the need to have a higher capital investment for technology that leads to better internal conditions.

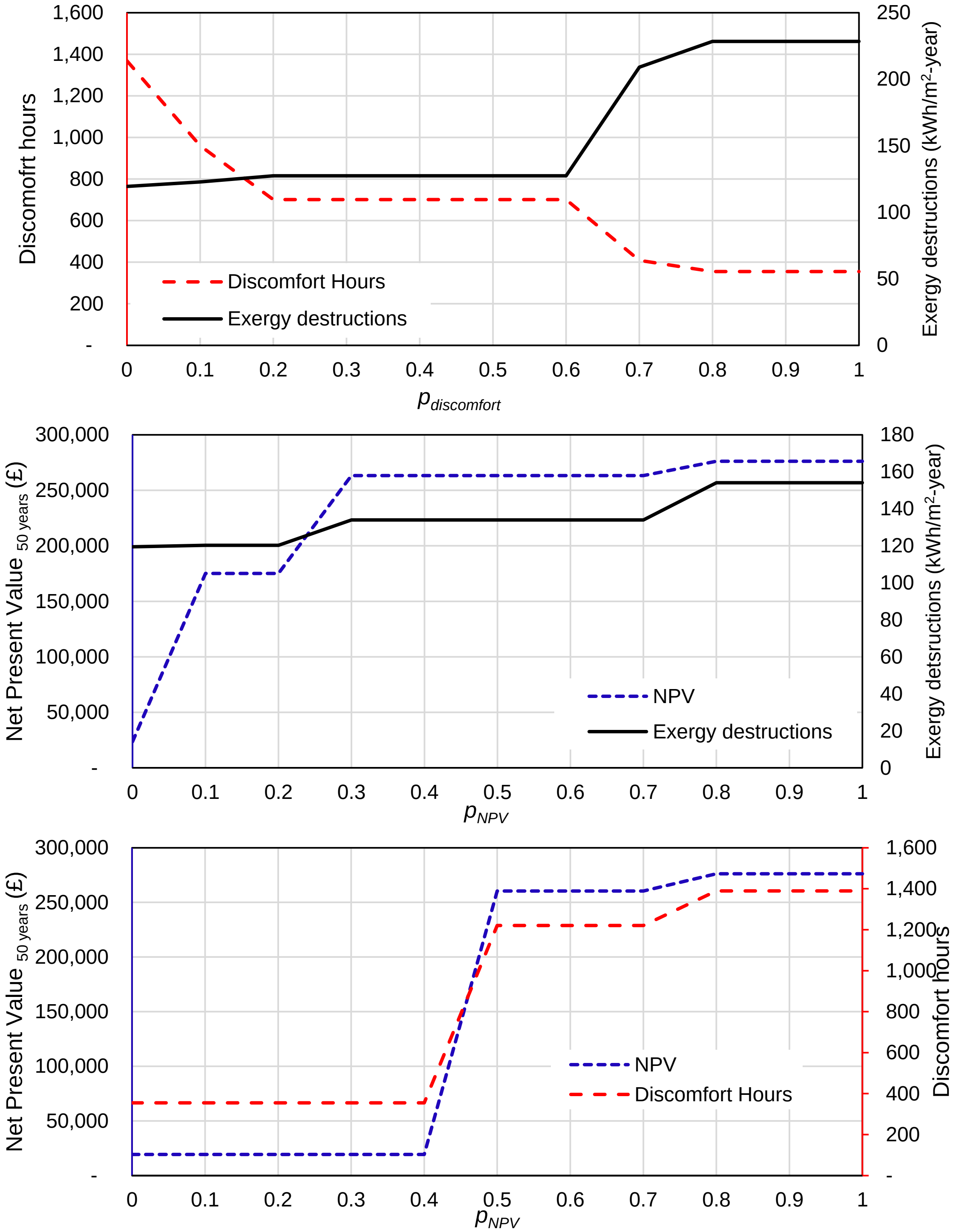

Fig. 21 Changes in the Primary School objective function values with respect to the weighting coefficient

6.5 Utopian solution vs baseline case

For a final comparison, the utopian solution is selected. The utopia point is a theoretical model which contains the minimum value for each of the three objectives optimised individually. To find this particular model, a weight coefficient with similar values has to be considered ($\boldsymbol{p}_{exergy\_dest}$ =0.33, $\boldsymbol{p}_{discomfort}$ =0.33, and $\boldsymbol{p}_{NPV}$ =0.33).

For the case study, the retrofitted model close to the utopia consists of an HVAC system H28: a 125 kW biomass-based condensing boiler connected to a low temperature wall heating system working with a heating set-point at 20 °C. The insulation for the wall is composed of Aerogel with a thickness of 0.015m, while the roof insulation is composed of 0.04m of phenolic board, and the ground of 0.12m of polyurethane. The infiltration rate keeps the baseline levels of 1.0 *ach*, while the glazing system is retrofitted with double-glazed, with a 6mm gap of Argon gas. For active systems, the lighting system is retrofitted to install T8 LEDs. Furthermore, the BER design does not consider any implementation of renewable electricity generation (PV or wind turbines). A schematic diagram of the building energy system in Fig. 22.

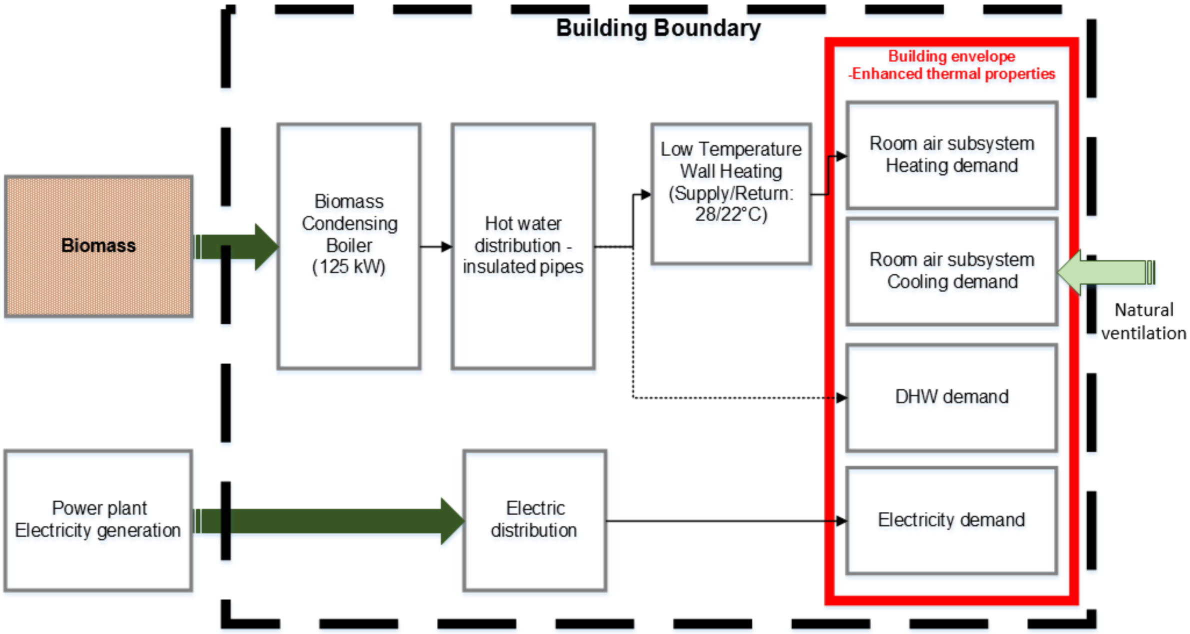

Fig. 22 Schematic layout of the energy system for the Primary School 'close to Utopia' BER model

From the baseline value of 187.9 kWh/m^2-year for energy use, the utopian model reduces it to 118.1 kWh/m^2-year. The utopian model compromises on greater energy use savings, as the optimisation process has a constraint to achieve a DPB of 50 years or less with a maximum budget of £734,968. This utopian model requires a retrofit capital cost of just £329,856, achieving a DPB of 49 years. Nevertheless, the utopian model improves on thermal comfort levels from a baseline value of 1,443 uncomfortable hours to 701 hours for the post-retrofit building. Additionally, the optimised design was able to reduce carbon emission baseline value up to 72.8%.

Notwithstanding, interesting outputs come from the exergy and exergoeconomic analyses. Fig. 23, showing that total exergy destruction rates are £1.38/h for the utopian model; representing a major improvement from the baseline case (£2.7/h). Moreover, BER capital cost rate - ***Z*** (in light red) and annual revenue rate - ***R*** (in light green) are illustrated for the utopian model. The utopian model achieves a ***Z*** of £1.41/h and an ***R*** of £1.47/h. When analysing the $Exec_{CB}$ indicator with the aim to find the best possible exergoeconomic design, this results in a value of £1.31/h, meaning that the obtained design provides better overall exergy/exergoeconomic performance compared to the pre-retrofitted building.

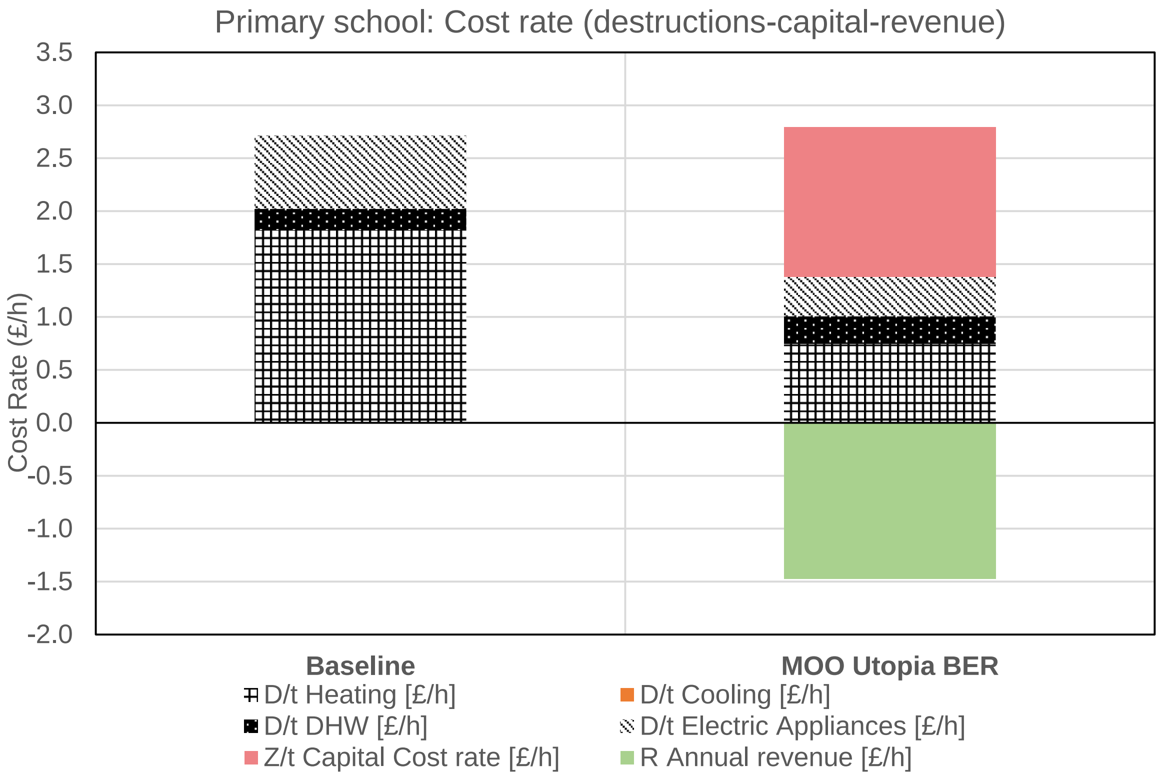

Fig. 23 Primary school exergy destruction, BER capital cost and annual revenue cost rate

The framework developed in this research has demonstrated to provide designs with an appropriate balance between active and passive measures, while consistently accounting for energy use, irreversibilities, and exergetic and economic costs along every subsystem in the building energy system. Meanwhile, the application of the exergoeconomic cost-benefit index could be a practical solution to supports building designers in making informed and robust economic decisions.

7. Conclusions

This paper presented ExRET-Opt, a retrofit-oriented simulation framework, which has become a part of EnergyPlus in performing exergy and exergoeconomic balances. The addition was done thanks to the development of external Python-based subroutines, and the support of the Java-based software jEPlus. ExRET-Opt, apart from providing the user with exergy data and pinpointing sources of inefficiencies along the energy supply chain, gives the possibility to perform a comprehensive exploration of a wide range state-of-the-art building energy technologies, with the intention to minimise energy use and improve thermodynamic efficiency of existing buildings. The retrofit technologies include high and low temperature HVAC systems, envelope insulation measures, insulated glazing systems, efficient lighting, energy renewable generation technologies, and set-points control measures. Moreover, integration of exergoeconomic analysis and multi-objective optimisation into EnergyPlus allows users to perform a comprehensive exergoeconomic optimisation similar to those found in the optimisation of chemical or power generation processes. It means that indicators such as energy, exergy, economic (capital cost, NPV), exergoeconomic, and carbon emissions combined with occupants' thermal comfort, can be used as constraints or objective functions in the optimisation procedure. The limited availability of robust and comprehensive test data has restricted the application of full validation tests to the results of ExRET-Opt. However, an inter-model and analytical verification processes was performed. By reviewing different existing exergy tools and exergy-based research, the calculation process of the two main subroutines developed for ExRET-opt, has been verified with acceptable results.

To demonstrate the strengths of ExRET-Opt in a real case study, the framework was applied to a school building. A hybrid-thermodynamic MOO problem, considering net present value (First Law), exergy destructions (Second Law), and occupant thermal comfort as objective functions was performed. Outputs demonstrate that by using exergy and NPV as objective functions it is possible to improve energy and exergy performance, reduce carbon and exergy destructions footprint, while also providing comfortable conditions under cost-effective solutions. This gives practitioners and decision makers more flexibility in the design process. Additionally, the results show that even with the imposed constraints, the NSGA-II-based MOO module was successfully applied, finding a large range of better performance BER designs for the analysed case study, compared with their corresponding baseline case. However, a tight (constrained) budget means missing out on some low-exergy systems, which require higher capital investment, such as district heating/cooling systems and ground source heat pumps. Finally, to compare the strength of an exergy-based MOO-MCDM, the utopian model was selected for a final comparison against the pre-retrofitted case. This solution represents the model closest to the optimal objectives, if they were optimised separately. These final selected solutions improved overall building's energy performance, exergy efficiency and buildings' life cycle cost while having low initial capital investments.

It is suggested that BER designs should result from a more holistic analysis. Exergy and exergoeconomics could have an important future role in the building industry if some practical barriers were overcome. The proposed methodological framework can provide more information than the typical optimisation methods based solely on energy analysis. The addition of exergy/exergoeconomic analysis to building optimisation completes a powerful and robust methodology that should be pursued in everyday BER practice. By utilising popular buildings' simulation tools as the foundation, practical exergy and exergoeconomics theory could become more accessible, reaching a wider audience of industry decision makers as well as academic researchers. Combined with other methods, such as multi-objective optimisation and multi criteria decision making, exergy finally could hold a good chance to find a place in the everyday practice.

Acknowledgments

The first author acknowledges support from The Mexican National Council for Science and Technology (CONACyT) through a scholarship to pursue doctoral studies with a CVU: 331698 and grant number: 217593.

Nomenclature

BER	building energy retrofit
$\dot{C}_D$	exergy destruction cost (£)
c_f	average cost of fuel (£/kWh)
c_p	average cost of product (£/kWh)
DPB	discounted payback (years)
EUI	energy use index (kWh/m²-year)
Ex	exergy (kWh)
$\dot{E}x_D$	exergy destructions (kWh)
$Exec_{CB}$	exergoeconomic cost benefit factor (£/h)
f_k	exergoeconomic factor (-)
NPV	net present value (£)
R	annual revenue (£)
TCI	total capital investment (£)
$\dot{Z}_k$	capital investment rate (£/h)
Greek symbols	
α_{cheb}	Chebyshev distance
ψ_{tot}	exergy efficiency (-)

Appendix A. Characteristics of building retrofit measures [58]

Table A.1 Characteristics and investment cost of HVAC systems

HVAC ID	System Description	Emission system	Cost
H1	*Condensing Gas Boiler + Chiller*	CAV	*Generation systems* • £160/kW Water-based Chiller (COP=3.2) • £99/kW Condensing gas boiler (η=0.95) • £70/kW Oil Boiler (η=0.90) • £150/kW Electric Boiler (η=1.0)
H2	*Condensing Gas Boiler + Chiller*	VAV	
H3	*Condensing Gas Boiler + ASHP-VRF System*	FC	
H4	*Oil Boiler + Chiller*	CAV	
H5	*Oil Boiler + Chiller*	VAV	
H6	*Oil Boiler + Chiller*	FC	
H7	*Electric Boiler + Chiller*	CAV	
H8	*Electric Boiler + Chiller*	VAV	

H9	*Electric Boiler + ASHP-VRF System*	FC	• £208/kW Biomass Boiler (η=0.90) • £1300/kW ASHP-VRF System (COP=3.2) • £1200/kW GSHP (Water-Water) System (COP=4.2) • £452/kW ASHP (Air-Air) (COP=3.2) • £2000/kW PV-T system • £27,080 micro-CHP (5.5 kW) + fuel cell system Emission systems • £700 per CAV • £1200 per VAV • £35/m² wall heating • £35/m² underfloor heating • £6117 per Heat Recovery system Other subsystems: • £56/kW District heat exchanger + £6122 connection charge • £50/m for building's insulated distribution pipes
H10	*Biomass Boiler + Chiller*	CAV	
H11	*Biomass Boiler + Chiller*	VAV	
H12	*Biomass Boiler + ASHP-VRF System*	FC	
H13	*District system*	CAV	
H14	*District system*	VAV	
H15	*District system*	Wall	
H16	*District system*	Underfloor	
H17	*District system*	Wall+Underfloor	
H18	*Ground Source Heat Pump*	CAV	
H19	*Ground Source Heat Pump*	VAV	
H20	*Ground Source Heat Pump*	Wall	
H21	*Ground Source Heat Pump*	Underfloor	
H22	*Ground Source Heat Pump*	Wall+Underfloor	
H23	*Air Source Heat Pump*	CAV	
H24	*PVT-based system (50% roof) with supplemental Electric boiler and Old Chiller*	CAV	
H25	*Condensing Boiler + Chiller*	Wall	
H26	*Condensing Boiler + Chiller*	Underfloor	
H27	*Condensing Boiler + Chiller*	Wall+Underfloor	
H28	*Biomass Boiler + Chiller*	Wall	
H29	*Biomass Boiler + Chiller*	Underfloor	
H30	*Biomass Boiler + Chiller*	Wall+Underfloor	
H31	*Micro-CHP with Fuel Cell and Electric boiler and old Chiller*	CAV	
H32	*Condensing Gas Boiler and old Chiller. Heat Recovery System included.*	CAV	

Table A.2 Characteristics and investment cost of lighting systems

Lights ID	Lighting technology	Cost per W/m²
L1	*T8 LFC*	£5.55
L2	*T5 LFC*	£7.55
L3	*T8 LED*	£11.87

Table A.3 Characteristics and investment cost of renewable energy generation systems

Renewable	Technology	Cost
R1	*PV panels 25% roof*	PV: £1200/m²
R2	*PV panels 50% roof*	
R3	*PV panels 75% roof*	
R4	*Wind Turbine 20 kW*	Turbine: £4000/kW
R5	*Wind Turbine 40 kW*	£/kW

Table A.4 Characteristics and investment cost of different insulation materials

Ins. ID	Insulation measure	Thickness (cm)	Total of measures	Cost per m² (lowest to highest)
I1	*Polyurethane*	2 to 15 in 1 cm steps	14	£6.67 to £23.32
I2	*Extruded polystyrene*	1 to 15 in 1 cm steps	15	£4.77 to £31.99
I3	*Expanded polystyrene*	2 to 15 in 1 cm steps	14	£4.35 to £9.95
I4	*Cellular Glass*	4 to 18 in 1 cm steps	15	£16.21 to £72.94

I5	*Glass Fibre*	6.7, 7.5, 8.5, and 10 cm	4	£5.65 to £7.75
I6	*Cork board*	2 to 6 in 1 cm steps, 8 to 20 cm in 2 cm steps, 28 and 30 cm	14	£5.57 to £85.80
I7	*Phenolic foam board*	2 to 10 in 1 cm steps	9	£5.58 to £21.89
I8	*Aerogel*	0.5 to 4 in 0.5 cm steps	8	£26.80 to £195.14
I9	*PCM (w/board)*	10 and 20 mm	2	£57.75 to £107.75

Table A.5 Characteristics and investment cost of glazing systems

Glazing ID	System Description (# panes – gap)	Gas Filling	Cost per m²
G1	*Double pane - 6mm*	Air	£261
G2	*Double pane - 13mm*	Air	£261
G3	*Double pane - 6mm*	Argon	£350
G4	*Double pane - 13mm*	Argon	£350
G5	*Double pane - 6mm*	Krypton	£370
G6	*Double pane - 13mm*	Krypton	£370
G7	*Triple pane - 6mm*	Air	£467
G8	*Triple pane - 13mm*	Air	£467
G9	*Triple pane - 6mm*	Argon	£613
G10	*Triple pane - 13mm*	Argon	£613
G11	*Triple pane - 6mm*	Krypton	£653
G12	*Triple pane - 13mm*	Krypton	£653

Table A.6 Characteristics and investment cost for air tightness improvement considering baseline of 1 ach

Sealing ID	ACH (1/h) Improvement %	Cost per m² (opaque envelope)
S1	*10%*	£1.20
S2	*20%*	£3.31
S3	*30%*	£6.35
S4	*40%*	£10.30
S5	*50%*	£15.20
S6	*60%*	£20.98
S7	*70%*	£27.69
S8	*80%*	£35.33
S9	*90%*	£43.88

Table A.7 Cooling and heating indoor set points variations

Set-point ID	Set-point Type	Value (°C)	Cost
SH18	*Heating*	18	(-)
SH19		19	
SH20		20	
SH21		21	
SH22		22	
SC23	*Cooling*	23	(-)
SC24		24	
SC25		25	
SC26		26	
SC27		27	

Appendix B. Multi-criteria decision making outputs

Table B-1 Sample of 'optimal solutions' obtained from Primary School Pareto front using Compromise Programming

p_{ex}	p_{com}	p_{NPV}	[min] α_{cheb}	$Ex_{dest,bui}$ (kWh/m^2-year)	*Discomfort* (hours)	$NPV_{50years}$ (£)	X^{HVAC} (Type)	X^{wall} (m)	X^{roof} (m)	X^{ground} (m)	X^{seal} (ach)	X^{glaz} (type)	X^{light} Light techn.	X^{PV} % roof panels	X^{wind} (kW)	X^{heat} (°C)
1	**0**	**0**	0.00	119.4	1,369	23,493	28	3.11	7.04	2.02	0.3	2	3	0	0	20
0.9	**0.1**	**0**	0.08	122.8	960	2,069	28	3.02	4.05	4.12	0.7	1	3	0	20	19
0.9	**0**	**0.1**	0.04	120.3	1,382	175,127	31	5.075	5.1	3.11	0.5	5	2	0	0	19
0.8	**0.2**	**0**	0.11	127.4	701	13,964	28	8.015	7.04	1.12	1	3	3	0	0	20
0.8	**0.1**	**0.1**	0.14	120.3	1,382	175,127	31	5.075	5.1	3.11	0.5	5	2	0	0	19
0.8	**0**	**0.2**	0.08	120.3	1,382	175,127	31	5.075	5.1	3.11	0.5	5	2	0	0	19
0.7	**0.3**	**0**	0.14	127.4	701	13,964	28	8.015	7.04	1.12	1	3	3	0	0	20
0.7	**0.2**	**0.1**	0.20	127.4	701	13,964	28	8.015	7.04	1.12	1	3	3	0	0	20
0.7	**0.1**	**0.2**	0.17	120.3	1,382	175,127	31	5.075	5.1	3.11	0.5	5	2	0	0	19
0.7	**0**	**0.3**	0.09	134.0	1,417	263,272	31	3.14	3.15	1.11	0.4	0	0	0	0	20
0.6	**0.4**	**0**	0.16	127.4	701	13,964	28	8.015	7.04	1.12	1	3	3	0	0	20
0.6	**0.3**	**0.1**	0.23	127.4	701	13,964	28	8.015	7.04	1.12	1	3	3	0	0	20
0.6	**0.2**	**0.2**	0.27	120.3	1,382	175,127	31	5.075	5.1	3.11	0.5	5	2	0	0	19
0.6	**0.1**	**0.3**	0.18	134.0	1,417	263,272	31	3.14	3.15	1.11	0.4	0	0	0	0	20
0.6	**0**	**0.4**	0.08	134.0	1,417	263,272	31	3.14	3.15	1.11	0.4	0	0	0	0	20
0.5	**0.5**	**0**	0.19	127.4	701	13,964	28	8.015	7.04	1.12	1	3	3	0	0	20
0.5	**0.4**	**0.1**	0.25	127.4	701	13,964	28	8.015	7.04	1.12	1	3	3	0	0	20
0.5	**0.3**	**0.2**	0.32	127.4	701	13,964	28	8.015	7.04	1.12	1	3	3	0	0	20
0.5	**0.2**	**0.3**	0.27	134.0	1,417	263,272	31	3.14	3.15	1.11	0.4	0	0	0	0	20
0.5	**0.1**	**0.4**	0.17	134.0	1,417	263,272	31	3.14	3.15	1.11	0.4	0	0	0	0	20
0.5	**0**	**0.5**	0.08	134.0	1,417	263,272	31	3.14	3.15	1.11	0.4	0	0	0	0	20
0.4	**0.6**	**0**	0.22	127.4	701	13,964	28	8.015	7.04	1.12	1	3	3	0	0	20
0.4	**0.5**	**0.1**	0.28	127.4	701	13,964	28	8.015	7.04	1.12	1	3	3	0	0	20
0.4	**0.4**	**0.2**	0.34	127.4	701	13,964	28	8.015	7.04	1.12	1	3	3	0	0	20
0.4	**0.3**	**0.3**	0.35	134.0	1,417	263,272	31	3.14	3.15	1.11	0.4	0	0	0	0	20
0.4	**0.2**	**0.4**	0.26	134.0	1,417	263,272	31	3.14	3.15	1.11	0.4	0	0	0	0	20
0.4	**0.1**	**0.5**	0.16	134.0	1,417	263,272	31	3.14	3.15	1.11	0.4	0	0	0	0	20
0.4	**0**	**0.6**	0.07	134.0	1,417	263,272	31	3.14	3.15	1.11	0.4	0	0	0	0	20
0.3	**0.7**	**0**	0.23	209.1	409	7,548	10	3.08	3.11	6.05	0.3	5	0	0	0	18
0.3	**0.6**	**0.1**	0.31	127.4	701	13,964	28	8.015	7.04	1.12	1	3	3	0	0	20
0.3	**0.5**	**0.2**	0.37	127.4	701	13,964	28	8.015	7.04	1.12	1	3	3	0	0	20

0.3	**0.4**	**0.3**	0.43	160.8	1,220	260,385	31	6.05	3.1	0	0.8	1	0	0	0	21
0.3	**0.3**	**0.4**	0.35	134.0	1,417	263,272	31	3.14	3.15	1.11	0.4	0	0	0	0	20
0.3	**0.2**	**0.5**	0.25	134.0	1,417	263,272	31	3.14	3.15	1.11	0.4	0	0	0	0	20
0.3	**0.1**	**0.6**	0.16	134.0	1,417	263,272	31	3.14	3.15	1.11	0.4	0	0	0	0	20
0.3	**0**	**0.7**	0.06	134.0	1,417	263,272	31	3.14	3.15	1.11	0.4	0	0	0	0	20
0.2	**0.8**	**0**	0.15	228.4	355	19,333	10	4.13	3.15	5.065	0.6	6	0	0	0	19
0.2	**0.7**	**0.1**	0.25	228.4	355	19,333	10	4.13	3.15	5.065	0.6	6	0	0	0	19
0.2	**0.6**	**0.2**	0.34	228.4	355	19,333	10	4.13	3.15	5.065	0.6	6	0	0	0	19
0.2	**0.5**	**0.3**	0.44	228.4	355	19,333	10	4.13	3.15	5.065	0.6	6	0	0	0	19
0.2	**0.4**	**0.4**	0.41	160.8	1,220	260,385	31	6.05	3.1	0	0.8	1	0	0	0	21
0.2	**0.3**	**0.5**	0.33	160.8	1,220	260,385	31	6.05	3.1	0	0.8	1	0	0	0	21
0.2	**0.2**	**0.6**	0.24	154.1	1,389	276,182	31	8.005	1.09	3.02	0.6	0	0	0	0	20
0.2	**0.1**	**0.7**	0.15	154.1	1,389	276,182	31	8.005	1.09	3.02	0.6	0	0	0	0	20
0.2	**0**	**0.8**	0.05	154.1	1,389	276,182	31	8.005	1.09	3.02	0.6	0	0	0	0	20
0.1	**0.9**	**0**	0.08	228.4	355	19,333	10	4.13	3.15	5.065	0.6	6	0	0	0	19
0.1	**0.8**	**0.1**	0.17	228.4	355	19,333	10	4.13	3.15	5.065	0.6	6	0	0	0	19
0.1	**0.7**	**0.2**	0.26	228.4	355	19,333	10	4.13	3.15	5.065	0.6	6	0	0	0	19
0.1	**0.6**	**0.3**	0.36	228.4	355	19,333	10	4.13	3.15	5.065	0.6	6	0	0	0	19
0.1	**0.5**	**0.4**	0.45	228.4	355	19,333	10	4.13	3.15	5.065	0.6	6	0	0	0	19
0.1	**0.4**	**0.5**	0.38	160.8	1,220	260,385	31	6.05	3.1	0	0.8	1	0	0	0	21
0.1	**0.3**	**0.6**	0.31	160.8	1,220	260,385	31	6.05	3.1	0	0.8	1	0	0	0	21
0.1	**0.2**	**0.7**	0.22	154.1	1,389	276,182	31	8.005	1.09	3.02	0.6	0	0	0	0	20
0.1	**0.1**	**0.8**	0.12	154.1	1,389	276,182	31	8.005	1.09	3.02	0.6	0	0	0	0	20
0.1	**0**	**0.9**	0.02	154.1	1,389	276,182	31	8.005	1.09	3.02	0.6	0	0	0	0	20
0	**1**	**0**	0.00	228.4	355	19,333	10	4.13	3.15	5.065	0.6	6	0	0	0	19
0	**0.9**	**0.1**	0.09	228.4	355	19,333	10	4.13	3.15	5.065	0.6	6	0	0	0	19
0	**0.8**	**0.2**	0.19	228.4	355	19,333	10	4.13	3.15	5.065	0.6	6	0	0	0	19
0	**0.7**	**0.3**	0.28	228.4	355	19,333	10	4.13	3.15	5.065	0.6	6	0	0	0	19
0	**0.6**	**0.4**	0.37	228.4	355	19,333	10	4.13	3.15	5.065	0.6	6	0	0	0	19
0	**0.5**	**0.5**	0.44	160.8	1,220	260,385	31	6.05	3.1	0	0.8	1	0	0	0	21
0	**0.4**	**0.6**	0.36	160.8	1,220	260,385	31	6.05	3.1	0	0.8	1	0	0	0	21
0	**0.3**	**0.7**	0.28	160.8	1,220	260,385	31	6.05	3.1	0	0.8	1	0	0	0	21
0	**0.2**	**0.8**	0.19	154.1	1,389	276,182	31	8.005	1.09	3.02	0.6	0	0	0	0	20
0	**0.1**	**0.9**	0.10	154.1	1,389	276,182	31	8.005	1.09	3.02	0.6	0	0	0	0	20
0	**0**	**1**	0.00	154.1	1,389	276,182	31	8.005	1.09	3.02	0.6	0	0	0	0	20

963

References

[1] Dincer I, Zamfirescu C. Sustainable Energy Systems and Applications. US: Springer 2012.

[2] Miller C, Hersberger C, Jones M. Automation of common building energy simulation workflows using python In: IBPSA editor. Conference Automation of common building energy simulation workflows using python, Chambery, France. p. 210-7.

[3] LBNL, USDOE. DOE-2. James J. Hirsch & Associates 2015.

[4] EnergyPlus. EnergyPlus Engineering Reference. 2012. p. 1278.

[5] Chuah JW, Raghunathan A, Jha NK. ROBESim: A retrofit-oriented building energy simulator based on EnergyPlus. Energy and Buildings. 2013;66(0):88-103.

[6] Hong T, Piette MA, Chen Y, Lee SH, Taylor-Lange SC, Zhang R, et al. Commercial Building Energy Saver: An energy retrofit analysis toolkit. Applied Energy. 2015;159:298-309.

[7] Mauro GM, Hamdy M, Vanoli GP, Bianco N, Hensen JLM. A new methodology for investigating the cost-optimality of energy retrofitting a building category. Energy and Buildings. 2015;107:456-78.

[8] Rysanek AM, Choudhary R. Optimum building energy retrofits under technical and economic uncertainty. Energy and Buildings. 2013;57(0):324-37.

[9] Klein SA. TRNSYS 17: A Transient System Simulation Program. In: Solar Energy Laboratory UoW, editor. Madison, USA2010.

[10] The MathWorks. MATLAB and Statistics Toolbox Release 2012b. Natick, Massachusetts, United States.2012.

[11] Nguyen A-T, Reiter S, Rigo P. A review on simulation-based optimization methods applied to building performance analysis. Applied Energy. 2014;113(0):1043-58.

[12] Attia S, Hamdy M, O'Brien W, Carlucci S. Assessing gaps and needs for integrating building performance optimization tools in net zero energy buildings design. Energy and Buildings. 2013;60(0):110-24.

[13] Siddharth V, Ramakrishna PV, Geetha T, Sivasubramaniam A. Automatic generation of energy conservation measures in buildings using genetic algorithms. Energy and Buildings. 2011;43(10):2718-26.

[14] Asadi E, da Silva MG, Antunes CH, Dias L. Multi-objective optimization for building retrofit strategies: A model and an application. Energy and Buildings. 2012;44(0):81-7.

[15] Malatji EM, Zhang J, Xia X. A multiple objective optimisation model for building energy efficiency investment decision. Energy and Buildings. 2013;61(0):81-7.

[16] Diakaki C, Grigoroudis E, Kolokotsa D. Towards a multi-objective optimization approach for improving energy efficiency in buildings. Energy and Buildings. 2008;40(9):1747-54.

[17] Tsatsaronis G. Exergoeconomics and Exergoenvironmental Analysis. In: Bakshi BR, Gutowski TG, Sekulic DP, editors. Thermodynamics and the Destruction of Resources: Cambridge University Press; 2014.

[18] Hammond GP, Stapleton AJ. Exergy analysis of the United Kingdom energy system. Proceedings of the Institution of Mechanical Engineers, Part A: Journal of Power and Energy. 2001;215(2):141-62.

[19] Gasparatos A, El-Haram M, Horner M. Assessing the sustainability of the UK society using thermodynamic concepts: Part 2. Renewable and Sustainable Energy Reviews. 2009;13(5):956-70.

[20] Streich M. Opportunities and limits for exergy analysis in cryogenics. Chemical Engineering & Technology. 1996;19:498-502.

[21] Lior N. Thoughts about future power generation systems and the role of exergy analysis in their development. Energy Conversion and Management. 2002;43:1187-98.

[22] Montelongo-Luna JM, Svrcek WY, Young BR. An exergy calculator tool for process simulation. Asia-Pacific Journal of Chemical Engineering. 2007;2:431-7.

[23] Querol E, Gonzalez-Regueral B, Ramos A, Perez-Benedito JL. Novel application for exergy and thermoeconomic analysis of processes simulated with Aspen Plus®. Energy. 2011;36:964-74.

[24] Suleman F, Dincer I, Agelin-Chaab M. Energy and exergy analyses of an integrated solar heat pump system. Applied Thermal Engineering. 2014;73:559-66.

[25] Ghannadzadeh A, Thery-Hetreux R, Baudouin O, Baudet P, Floquet P, Joulia X. General methodology for exergy balance in ProSimPlus® process simulator. Energy. 2012;44:38-59.

[26] Fisk D. Optimising heating system structure using exergy Branch and Bound. Building Services Engineering Research and Technology. 2014;35(3):321-33.

[27] EBC-Annex37. Technical Synthesis Report: Low Exergy Systems for Heating and Cooling of Buildings, IEA ECBCS. In: Jagpal R, editor. UK2007.

[28] Sakulpipatsin P, Schmidt D. Exergy analysis applied to building design. 2005:8.

[29] EBC-Annex49. Detailed Exergy Assessment Guidebook for the Built Environment, IEA ECBCS. In: Torio H, Schmidt D, editors.: Fraunhofer IBP; 2011.

[30] Schlueter A, Thesseling F. Building information model based energy/exergy performance assessment in early design stages. Automation in Construction. 2009;18(2):153-63.

[31] Sakulpipatsin P, Itard LCM, van der Kooi HJ, Boelman EC, Luscuere PG. An exergy application for analysis of buildings and HVAC systems. Energy and Buildings. 2010;42(1):90-9.

[32] Angelotti A, Caputo P, Solani G. Dynamic exergy analysis of an air source heat pump. 1st International Exergy, Life Cycle Assessment, and Sustainability Workshop & Symposium (ELCAS). 2009:8.

[33] Tsatsaronis G, Park M-H. On avoidable and unavoidable exergy destructions and investment costs in thermal systems. Energy Conversion and Management. 2002;43:1259-70.

[34] Rocco MV, Colombo E, Sciubba E. Advances in exergy analysis: a novel assessment of the Extended Exergy Accounting method. Applied Energy. 2014;113:1405-20.

[35] Wall G. Exergy - a useful concept within resource accounting. 1977(Report no. 77-42, Institute of Theoretical Physics, Chalmers University of Technology and University of Göteborg).

[36] Kohl T, Teles M, Melin K, Laukkanen T, Järvinen M, Park SW, et al. Exergoeconomic assessment of CHP-integrated biomass upgrading. Applied Energy. 2015;156:290-305.

[37] Mosaffa AH, Garousi Farshi L. Exergoeconomic and environmental analyses of an air conditioning system using thermal energy storage. Applied Energy. 2016;162:515-26.

[38] Wang X, Dai Y. Exergoeconomic analysis of utilizing the transcritical CO2 cycle and the ORC for a recompression supercritical CO2 cycle waste heat recovery: A comparative study. Applied Energy. 2016;170:193-207.

[39] Valero A, Torres C. Thermoeconomic Analysis. In: Frangopoulosaylo CA, editor. Exergy, energy system analysis, and optimization: EOLSS; 2009. p. 454.

[40] Valdés M, Durán MD, Rovira A. Thermoeconomic optimization of combined cycle gas turbine power plants using genetic algorithms. Applied Thermal Engineering. 2003;23:2169-82.

[41] Mofid G-B, Hamed G. Exergoeconomic optimization of gas turbine power plants operating parameters using genetic algorithms: A case study. Thermal Science 2011;15:43-54.

[42] Ahmadi P, Dincer I, Rosen MA. Thermodynamic modeling and multi-objective evolutionary-based optimization of a new multigeneration energy system. Energy Conversion and Management. 2013;76:282-300.

[43] Dong R, Yu Y, Zhang Z. Simultaneous optimization of integrated heat, mass and pressure exchange network using exergoeconomic method. Applied Energy. 2014;136:1098-109.

[44] Sadeghi M, Chitsaz A, Mahmoudi SMS, Rosen MA. Thermoeconomic optimization using an evolutionary algorithm of a trigeneration system driven by a solid oxide fuel cell. Energy. 2015;89:191-204.

[45] Baghsheikhi M, Sayyaadi H. Real-time exergoeconomic optimization of a steam power plant using a soft computing-fuzzy inference system. Energy. 2016;114:868-84.

[46] Deslauriers M-A, Sorin M, Marcos B, Richard M-A. Retrofit of low-temperature heat recovery industrial systems using multiobjective exergoeconomic optimization. Energy Conversion and Management. 2016;130:207-18.

[47] Xia J, Wang J, Lou J, Zhao P, Dai Y. Thermo-economic analysis and optimization of a combined cooling and power (CCP) system for engine waste heat recovery. Energy Conversion and Management. 2016;128:303-16.

[48] Ozcan H, Dincer I. Exergoeconomic optimization of a new four-step magnesium–chlorine cycle. International Journal of Hydrogen Energy. 2017.

[49] Tozer R, Lozano Serrano MA, Valero Capilla A, James R. Thermoeconomics applied to an air conditioning system with cogeneration. Building Services Engineering Research and Technology. 1996;17(1):37-42.

[50] Tozer R, James R. Thermoeconomic life-cycle costs of absorption chillers. Building Services Engineering Research and Technology. 1997;18(3):149-55.

[51] Ozgener O, Hepbasli A, Dincer I, Rosen MA. Modelling and assessment of ground-source heat pump systems using exergoeconomic analysis for building applications. Ninth International IBPSA Conference Montréal, Canada. 2005:15–8.

[52] Ucar A. Thermoeconomic analysis method for optimization of insulation thickness for the four different climatic regions of Turkey. Energy. 2010;35(4):1854-64.

[53] Caliskan H, Dincer I, Hepbasli A. Thermoeconomic analysis of a building energy system integrated with energy storage options. Energy Conversion and Management. 2013;76(0):274-81.

[54] Baldvinsson I, Nakata T. A comparative exergy and exergoeconomic analysis of a residential heat supply system paradigm of Japan and local source based district heating system using SPECO (specific exergy cost) method. Energy. 2014;74:537-54.

[55] Yücer CT, Hepbasli A. Exergoeconomic and enviroeconomic analyses of a building heating system using SPECO and Lowex methods. Energy and Buildings. 2014;73(0):1-6.

[56] Akbulut U, Utlu Z, Kincay O. Exergoenvironmental and exergoeconomic analyses of a vertical type ground source heat pump integrated wall cooling system. Applied Thermal Engineering. 2016;102:904-21.

[57] García Kerdan I, Raslan R, Ruyssevelt P. An exergy-based multi-objective optimisation model for energy retrofit strategies in non-domestic buildings. Energy. 2016;117, Part 2:506-22.

[58] García Kerdan I, Raslan R, Ruyssevelt P, Morillón Gálvez D. An exergoeconomic-based parametric study to examine the effects of active and passive energy retrofit strategies for buildings. Energy and Buildings. 2016;133:155-71.

[59] Torio H. Comparison and optimization of building energy supply systems through exergy analysis and its perspectives: Fraunhofer, 2012.

[60] Rosen M, Bulucea CA. Using Exergy to Understand and Improve the Efficiency of Electrical Power Technologies. Entropy. 2009;11(4):820-35.

[61] Lazzaretto A, Tsatsaronis G. SPECO: A systematic and general methodology for calculating efficiencies and costs in thermal systems. Energy. 2006;31(8–9):1257-89.

[62] Tsatsaronis G. Thermoeconomic analysis and optimization of energy systems. Progress in Energy and Combustion Science. 1993;19(3):227-57.

[63] Ma Z, Cooper P, Daly D, Ledo L. Existing building retrofits: Methodology and state-of-the-art. Energy and Buildings. 2012;55(0):889-902.

[64] SimLab 2.2. Simulation environment for uncertainty and sensitivity analysis. . Joint Research Center of the European Commission.; 2011.

[65] Python Software Foundation. Python Language Reference version 2.7.

[66] jEPlus 1.6. JEPlus – An EnergyPlus simulation manager for parametrics. 2016.

[67] jEPlus+EA 1.7. Building Design Optimization using jEPlus. 2016.

[68] CIBSE. Guide A: Environmental Design. In: Engineers CIoBS, editor. London, UK2015.

[69] ASHRAE. ANSI/ASHRAE Standard 55-2004. Thermal Environmental Conditions for Human Occupancy. American Society of Heating, Refrigerating and Air-conditioning Engineers; 2004.

[70] Korolija I, Marjanovic-Halburd L, Zhang Y, Hanby VI. UK office buildings archetypal model as methodological approach in development of regression models for predicting building energy consumption from heating and cooling demands. Energy and Buildings. 2013;60(0):152-62.

[71] CIBSE. Guide F: Energy Efficiency in Buildings. In: Engineers CIoBS, editor. London, UK2012.

[72] ARUP. Low Carbon Routemap for the UK Built Environment. In: Board TGC, editor. UK2013.

[73] Haupt RL, Haupt SE. Practical Genetic Algorithms. 2nd ed: Wiley, 2004.

[74] BRE. National Calculation Methodology (NCM) modelling guide (for buildings other than dwellings in England and Wales). 2010 Edition. In: (BRE, editor. Department for Communities and Local Government2013. p. 34.

[75] Bull J, Gupta A, Mumovic D, Kimpian J. Life cycle cost and carbon footprint of energy efficient refurbishments to 20th century UK school buildings. International Journal of Sustainable Built Environment. 2015.